JYVÄSKYLÄ STUDIES IN COMPUTING
66

Rui Wu

Methods for Space-Time Parameter Estimation in DS-CDMA arrays

JYVÄSKYLÄN YLIOPISTO

JYVÄSKYLÄ STUDIES IN COMPUTING 66

Rui Wu

Methods for Space-Time Parameter Estimation in DS-CDMA arrays

Esitetään Jyväskylän yliopiston informaatioteknologian tiedekunnan suostumuksella
julkisesti tarkastettavaksi yliopiston Villa Ranan Blomstedtin salissa
joulukuun 8. päivänä 2006 kello 12.

Academic dissertation to be publicly discussed, by permission of
the Faculty of Information Technology of the University of Jyväskylä,
in the Building Villa Rana, Blomstedt Hall, on December 8, 2006 at 12 o'clock noon.

UNIVERSITY OF JYVÄSKYLÄ

JYVÄSKYLÄ 2006

Methods for Space-Time Parameter Estimation in DS-CDMA arrays

JYVÄSKYLÄ STUDIES IN COMPUTING 66

Rui Wu

Methods for Space-Time Parameter Estimation in DS-CDMA arrays

UNIVERSITY OF JYVÄSKYLÄ

JYVÄSKYLÄ 2006

Editors
Tommi Kärkkäinen
Department of Mathematical Information Technology, University of Jyväskylä
Pekka Olsbo, Marja-Leena Tynkkynen
Publishing Unit, University Library of Jyväskylä

URN:ISBN:9513926958
ISBN 951-39-2695-8 (PDF)

ISBN 951-39-2629-X (nid.)
ISSN 1456-5390

Jyväskylä University Printing House, Jyväskylä 2006

ABSTRACT

Wu, Rui
Methods for Space-Time Parameter Estimation in DS-CDMA arrays
Jyväskylä: University of Jyväskylä, 2006, 73 p.
(Jyväskylä Studies in Computing
ISSN 1456-5390; 66)
ISBN 951-39-2695-8
Diss.

To improve spectrum efficiency and increase link quality, the usage of antenna array at the base station is a promising approach for the rapid growth of wireless communication. To take full advantage of the multiple antennas, space-time signal processing techniques need to be developed. For these techniques, a key aspect is the estimation of channel and channel parameters. Wireless signal propagation often exhibits a specular multipath. The estimation of direction-of-arrival (DOA) and/or time delay can be improved by the underlying structure of propagated signals. Improved channel estimation can result in improved signal-to-noise ratio (SNR), channel equalization, co-channel interference rejection and mobile localization. These in turn yield improved network performance.

In this thesis, we focus on the joint time delay and DOA estimation called two-dimensional code acquisition. Two classic algorithms are exploited for two-dimensional code acquisition. They are independent component analysis (ICA) and eigenvalue-eigenvector training support (EV-t) algorithms. ICA is a high order statistical technique. The benefit of using ICA for two-dimensional code acquisition is that it can effectively combat the near-far problem. In this thesis, ICA is further exploited for the fading problem. Before ICA is used to perform the two-dimensional code acquisition, interfering signals are suppressed by a preprocessor. The developed EV-t algorithm is a subspace based method which relies on eigenvalue-eigenvector decomposition and training sequence support. It mainly deals with the two-dimensional code acquisition in a high-correlated/coherent multi-path environment.

Keywords: DS-CDMA, two-dimensional code acquisition, DOA, time delay, ICA, EV-t

Author

Rui Wu
Department of Mathematical Information Technology
University of Jyväskylä
Finland

Supervisor

Professor Tapani Ristaniemi
Department of Mathematical Information Technology
University of Jyväskylä
Finland

Reviewers

Professor Olli Simula
Department of Computer Science and Engineering
Helsinki University of Technology
Finland

Professor Corneliu Marinov
Department of Electrical Engineering
Polytechnic University of Bucharest
Romania

Opponent

Professor Liviu Goras
Faculty of Electronics and Telecommunications
Technical University of Iasi
Romania

ACKNOWLEDGEMENTS

I am very thankful to my supervisor Professor Tapani Ristaniemi for his continuous research support and patience over the years. The guidance and encouragement he gave me during the work of this thesis means a great deal to me. His sharp observation and creative feedback inspired me throughout the course of the research.

My sincere gratitude goes to Professor Jyrki Joutsensalo who introduced me to the research area. He gave me valuable help during the beginning of the Ph.D. study. I would like to thank my reviewers Professor Olli Simula, Department of Computer Science and Engineering, Helsinki University of Technology, and Professor Corneliu Marinov, Polytechnic University of Bucharest, for their thorough examination of the manuscript.

I am indebted to the Graduate School in Computing and Mathematical Sciences (COMAS) at the University of Jyväskylä, and especially to the Academy of Finland for their financial support during the years of study. These foundations are greatly acknowledged for making the possibility to pursue my Ph.D. degree.

Finally, I would like to dedicate this thesis to my family. Over the past years, my husband, my son, and my daughter, their love, encouragement, expectation, and patience have made this thesis publishable. Furthermore, my thanks go to all my friends who have provided me with all kinds of help. Especially I would like to thank Xiawen Xie and Jing Wang, my honest friends, who gave me valuable hands at critical time of my life.

Jyväskylä, Finland

November 8, 2006

Rui Wu

SYMBOLS

$a_{k,l}(a_{k,l,i})$	attenuation factor of kth user lth path (for ith symbol)
$\mathbf{a}_{k,l}$	array response vectors of the space-time array model
$\mathbf{a}(\theta)$	array response vectors of the space array model
$\mathbf{A}$	matrix containing the attenuation factors $a_{k,l}$
$\mathbf{A}_i$	matrix containing the attenuation factors $a_{k,l,i}$
$\mathbf{A}(\theta)$	space array manifold
$b_{k,i}$	ith symbol transmitted by kth user
$\mathbf{b}_i$	symbol vector
$\mathbf{B}$	symbol matrix
c	speed of light
C_{bd}	coherence bandwidth
$\underline{\mathbf{c}}_{k,l}, \mathbf{c}_{k,l}, \overline{\mathbf{c}}_{k,l}$	code vectors corresponding to $\tau_{k,l}$
C_T	coherence time
d_u	space distance of a uniform linear array
D	dimension of the signal subspace
$\mathcal{D}$	slant range between a transmitter and a receiver
$E\{\cdot\}$	expectation operator
f_c	carrier frequency
f_D	maximum Doppler frequency shift
$\mathcal{F}$	fourier transform matrix
$\underline{\mathbf{g}}_{k,l}\mathbf{g}_{k,l}\overline{\mathbf{g}}_{k,l}$	code vectors corresponding to $h_{k,l}$
g_r	receiver gain
g_t	transmitter gain
$h_{k,l}$	integer part of a time delay
h_r	antenna height of a transmitter
h_t	antenna height of a receiver
$\underline{\mathbf{h}}_{k,l}\mathbf{h}_{k,l}\overline{\mathbf{h}}_{k,l}$	space-time response vectors
$(\cdot)^H$	complex conjugate transpose
$\mathbf{H}$	space-time array manifold
I	symbol number
$\mathbf{I}$	identify matrix
$\mathbf{J}$	mixing matrix of the linear ICA data model
K	user number
L	path number
$\mathbf{n}_i$	noise vector of the space-time array model
$\mathbf{n}(t)$	noise vector of the space array model
N	processing gain of the spreading code $s_k(\cdot)$
N_{R_s}	level crossing rate
$\mathbf{N}$	noise matrix
$\delta_{i,j}$	discrete kronecker delta function
θ	angle of arrival
ϕ_k	random carrier phase

$\otimes$	kronecker product
$\rho_{k(l,l')}$	correlation coefficient between the various paths
ρ_s	correlation coefficient between two array response vectors
$\underline{\rho}_{CV-(\cdot)}, \rho_{CV-(\cdot)}, \overline{\rho}_{CV-(\cdot)}$	correlation coefficients between two code vectors
$\underline{\rho}_{STV-(\cdot)}, \rho_{STV-(\cdot)}, \overline{\rho}_{STV-(\cdot)}$	correlation coefficients between two space-time response vectors
P_k	signal power of user k
$\mathbf{r}_i$	received data of the space-time array model
$\mathbf{R}_r$	ensemble correlation matrix of $\mathbf{r}_i$
$\hat{\mathbf{R}}_r$	sampled correlation matrix of $\mathbf{r}_i$
$\mathbf{R}_{f(i)}$	correlation matrix of $\mathbf{f}_i$
$\mathbf{R}_{A(i)}$	correlation matrix of $\mathbf{A}_i$
$s_k(\cdot)$	spreading code of kth user
$\mathbf{s}_i$	source vector of the linear ICA data model
$\mathbf{s}(t)$	source vector of the space array model
T	symbol period
$\mathbf{T}$	un-mixing matrix
T_c	chip period
T_f	fade duration
T_m	maximum excess delay
$\zeta_{k,l}$	fractional part of a time delay
$\tau_{k,l}$	time delay
$(\cdot)^T$	transpose operation
λ	eigenvalue
$\hat{\lambda}$	estimated eigenvalue
$\dot{\lambda}$	noise free eigenvalue
$\mathbf{u}$	eigenvector
$\hat{\mathbf{u}}$	estimated eigenvector
$\mathbf{U}$	matrix of the eigenvectors
$\mathbf{U}_s$	matrix of the signal subspace eigenvectors
$\mathbf{U}_n$	matrix of the noise subspace eigenvectors
$\hat{\mathbf{U}}$	matrix of the estimated eigenvectors
$\hat{\mathbf{U}}_s$	matrix of the estimated signal subspace eigenvectors
$\hat{\mathbf{U}}_n$	matrix of the estimated noise subspace eigenvectors
v	velocity(m/sec)
$\mathbf{V}$	whitening matrix
$\mathbf{w}_{BF}$	weight vector of the conventional standard beamformer
w_c	carrier wavelength

$\mathbf{w}_{CAP}$	weight vector of the conventional capon's minimum variance method
$\mathbf{w}_{EV-t}$	weight vector of the EV-t algorithm
$\mathbf{w}_{ST-BF}$	weight vector of the space-time standard beamformer
$\mathbf{w}_{ST-CAP}$	weight vector of the space-time capon's minimum variance method
$\mathbf{x}_i$	observed signals of the linear ICA data model
$\mathbf{x}(t)$	observed signals of the space array model
$\mathbf{y}_i$	whitened matrix
$\mathbf{y}_{s(i)}$	whitenned matrix in the signal subspace
$\Pi(t)$	a unit rectangular pulse
η	bias
$(\cdot)^*$	complex conjugate operation

ABBREVIATIONS

MF	matched filter
BPSK	binary phase-shift keying
BSS	blind source separation
CRLB	cramer-rao lower bound
DFT	discrete fourier transform
DOA	direction-of-arrival
DML	deterministic maximum likelihood
DS − CDMA	direct-sequence code division multiple access
ESPRIT	estimation of signal parameters via rotational invariance techniques
EV	eigenvector estimator
EV − t	eigenvalue-eigenvector training support
ICA	independent component analysis
ICA − FS	independent component analysis frequency selection
ISI	inter-symbol interference
JADE − ESPRIT	joint angle and delay estimation-ESPRIT
LOS	line-of-sight
MAI	multiple access interference
Min − Norm	minimum norm
ML	maximum likelihood
MODE	method of direction estimation
MUSIC	multiple signal classification
MVDR	minimum variance distortionless response
NLOS	non-line-of-sight
PCA	principle component analysis
SI − JADE	shift-invariance joint angle and delay estimation
SML	stochastic maximum likelihood
SVD	singular value decomposition
TLS − ESPRIT	total least squares-ESPRIT
WSF	weight subspace fitting

CONTENTS

1 INTRODUCTION

1.1 Motivation

In communication systems, parameter estimation is a general pre-requisite task to facilitate the recovery of transmitted data of each user. The conventional matched filter (MF), maximum likelihood (ML) method, and subspace based methods etc. are well known for estimating the unknown signal parameters [47]. Subspace based methods are frequently considered as high resolution algorithms for parameter estimation. They are based on the eigen-decomposition of an array correlation matrix and formulate the parameter estimation in the signal or the noise subspace. Initially, subspace based methods were extensively studied in a space array model for directions-of-arrival (DOA) estimation. The instantaneous space array model is given as

$$\mathbf{x}(t) = \mathbf{A}(\theta)\mathbf{s}(t) + \mathbf{n}(t) \ . \tag{1}$$

By introducing the data vector $\mathbf{x}(t)$ for the observed signals, and the source vector $\mathbf{s}(t)$ for the source signals, the matrix $\mathbf{A}(\theta)$ denotes the array manifold. $\mathbf{n}(t)$ is the additive noise.

With the rapidly growing popularity of wireless communication, direct-sequence code division multiple access (DS-CDMA) technique [42] [76] has been exploited to improve spectrum utilization. As multiple users share the same frequency band, channel interferences, e.g. multiple access interference (MAI) and inter-symbol interference (ISI), cause performance and capacity degradations. To effectively reduce channel interferences, multiuser detectors [75] and conventional single user detectors, e.g. [46], with power control have been proposed. The accurate temporal information, referred to as time delay, is the main pre-requisite task for the detectors to suppress interferences [38] [39]. To completely cancel channel interferences, smart antennas are also widely studied [1] [14] [28] [32]. By exploiting the spatial structure of the received signals, a further interference suppression is performed. As a space-time array model is exploited [41], the array response vector in the space array model is replaced by the space-time response vector indexed by time delay and DOA. In this situation, joint time de-

lay and DOA estimation, called two-dimensional code acquisition, can be seen. The two-dimensional code acquisition is often mentioned to have a number of advantages [48]:

1) It can provide more accurate information than only a temporal or spatial parameter estimation,

2) when several set of parameters are estimated, the one associated with the smallest delay is the most probable portable direction, and

3) as the space-time array model is explored, the space-time manifold can be made into a a full rank matrix by increasing the number of antenna elements and the processing gain. This leads to the situation that the number of received signals can be significantly larger than the number of antenna elements.

1.2 Focuses of the thesis

Due to several essential benefits listed above, the scope of this thesis is to develop and apply algorithms for two-dimensional code acquisition in the DS-CDMA array model.

In DS-CDMA communication systems, all users concurrently use the same frequency band. The users are distinguished by assigning each user a unique code sequence upon which the data sequence to be transmitted is overlayed. Due to asynchronous transmission, the orthogonality among the users' received code sequences cannot in general be achieved. Hence, the inherent MAI problem arises. In this thesis, one focus is on devoting algorithms for two-dimensional code acquisition based on ICA, which mitigates the MAI problem.

In wireless communication systems, there are three distinct multipath propagation environments which can be classified as: uncorrelated, correlated, and coherent. A severe performance degradation can be caused by the high-correlated/-coherent signal propagation when subspace based methods, e.g. multiple signal classification (MUSIC), are used to perform the DOA estimation in the space array model [62]. Although weight subspace fitting (WSF) [78] and method of direction estimation (MODE) [65] are proposed to combat the deleterious effect due to the coherency in the space array model for DOA estimation, the two algorithms require priori knowledge of the number of coherent and non-coherent signals which are normally unknown. Meanwhile, spatial smoothing [61] and forward and backward spatial smoothing [43] [44] have also been proposed for DOA estimation to deal with the coherency problem in the space array model. They require a large number of antenna elements. Hence, another focus of the thesis is on resolving the performance degradation due to the high-correlated/coherent multipath propagation problem for two-dimensional code acquisition in the DS-CDMA array model regardless of the correlation between the various propagated paths.

1.3 Contribution

Two main categorial algorithms, independent component analysis (ICA) and eigenvalue-eigenvector training support (EV-t), are developed and applied for two-dimensional code acquisition in the DS-CDMA array model.

Firstly, this thesis applies a semi-blind method based on ICA for two-dimensional code acquisition. ICA is a high order statistical technique. Initially, it is utilized for a blind source separation problem (BSS). Here ICA is exploited for two-dimensional code acquisition with a high MAI suppression capability. However, in addition to the MAI problem, fading channel is also a serious challenge in wireless communication systems. As a solution, ICA is further developed for the problem. Namely, a pre-processing operation is performed to suppress MAI before applying ICA for two-dimensional code acquisition. The pre-processing operation relaxes the limitation of the standard ICA which does not work well in the fading channel.

Secondly, this thesis proposes a method called EV-t for two-dimensional code acquisition to solve the performance degradation due to the high-correlated/-coherent multipath propagation problem. To distinguish the general subspace based methods, EV-t looks for a maximum projection of the desired signal's space-time response vector on the signal subspace and searches the training sequence support which is assumed to be available. In the work of this thesis, the performance of the EV-t algorithm for two-dimensional code acquisition is analyzed both analytically and numerically. The simulation results show EV-t is robust for two-dimensional code acquisition regardless the correlation between the various propagated paths. Meanwhile, it is an effective method to perform the two-dimensional code acquisition in a high MAI environment even with a small received set of samples (symbols).

1.4 List of publications

This thesis consists of one journal paper and six conference papers for two-dimensional code acquisition. In addition, Section 4.4 of the thesis contains unpublished results.

I. R. Wu, T. Ristaniemi, "Joint Time Delay and DOA Estimation in CDMA Communication Using FastICA Algorithm", In *Proceedings of the 8th International Conference on Cellular and Intelligent Communications(CIC 2003)*, Oct. 28-31, 2003, Seoul, Korea.

II. T. Ristaniemi, R. Wu, "Interference Suppression for Spatial-Temporal Propagation Parameters Identification in Wireless Communications", In *Proceedings of the IEEE Communications, Circuits and Systems Conference (ICCCAS'04)*, pp. 1022-1026, June 27-29, 2004, Chengdu, China.

III. R. Wu, T. Ristaniemi, "Spatial-Temporal Propagation Parameter Estimation in the Asynchronous DS-CDMA Systems over Fading Channel", In *Proceedings of the IEEE Communications and Information Technologies Symposium (ISCIT 2004)*, pp. 166-170, Oct. 26-29, 2004, Sapporo, Japan.

IV. R. Wu, T. Ristaniemi, "EV-t Method for Parameter Estimation in DS-CDMA Communications", In *Proceedings of the Third IEEE International Workshop on Intelligent Signal Processing (WISP'2005)*, pp. 328-333, Sep. 1-3, 2005, Faro, Portugal.

V. R. Wu, T. Ristaniemi, "Semi-Blind Two-Dimensional Code Acquisition in CDMA Communications", *International Journal of Signal Processing*, Vol. 3, No. 1, pp. 30-38, 2006.

VI. R. Wu, T. Ristaniemi, "The Performance Analysis of EV-t method for Two-Dimensional Code Acquisition", In *Proceedings of the First IEEE Workshop on Computational Advances in Multi-Sensor Adaptive Processing (CAMSAP'2005)*, pp. 229-232, Dec. 13-15, 2005, Puerto Vallarta, Jalisco State, Mexico.

VII. R. Wu, T. Ristaniemi, "Performance Comparison of EV-t and MUSIC for Two-Dimensional Code Acquisition", In *Proceedings of IEEE International Symposium on Wireless Pervasive Computing 2006 (ISWPC'06)*, pp. 1-5, Jan. 16-18, 2006, Phuket, Thailand.

1.4.1 Author's contribution to the included publications

In publication I, the author has extended the idea of FastICA algorithm for two-dimensional code acquisition, and written the paper. The used algorithm in publication II has been explored by the author. Meanwhile, the author has contributed the first version of the paper. The simulation test of publication III has been completed by the provided fading channel simulation program from the coauthor. The author has done most of the writing of the paper.

In publications IV-VII, the author has developed the algorithm and analyzed the performance of the algorithm, and was mainly responsible for writing the papers.

In the publications above, the author has written simulation programs. All of the simulation tests for all of the original publications of the thesis have been run and analyzed by the author. The coauthor has finalized the writing of the above papers.

1.4.2 Other publications

During the course of the work, other publications have also been published, which are not included in the thesis. These publications include three conference papers and one US patent application.

1. R. Wu, T. Ristaniemi, "Estimation of Arrival Direction in Asynchronous DS-CDMA Systems", In *Proceedings of the 8th International Conference on Cellular and Intelligent Communications(CIC 2003)*, Oct. 28-31, 2003, Seoul, Korea.

2. T. Ristaniemi, R. Wu, "On the Performance of Multi-sensor Reception

in CDMA by Fast Independent Component Analysis", In *Proceedings of the IEEE Semiannual Vehicular Technology Conference (VTC2001 Spring)*, pp. 1829-1833, May 6-9, 2001, Rhodes, Greece.

3. T. Ristaniemi, R. Wu, "Mitigation of Continuous-wave Jamming in DS-CDMA Systems Using Blind Source Separation Techniques", In *Proceedings of 3rd International Conference on Independent Component Analysis and Blind Signal Separation (ICA 2001)*, pp. 716-721, Dec. 9-12, 2001, San Diego, California, USA.

4. R. Wu, T. Ristaniemi, "Method for Identifying Spatial-Temporal Propagation Parameters of DS-CDMA Array Signal", *US patent application*, 20055452, Aug. 25, 2005.

1.5 Organization of the thesis

The thesis is organized as follows.

Firstly in Chapter 2, some very general wireless communication issues, e.g. multipath propagation characteristics, are introduced. Then, the signal transmission and reception models are presented, and a space-time array model describing the physics of radio wave propagation is established. Furthermore, some basic assumptions for the parameters are discussed.

In Chapter 3, we take a view on a class of algorithms for parameter estimation, and especially pay attention to the existing algorithms for two-dimensional code acquisition.

In Chapter 4, the concept of ICA and its application for two-dimensional code acquisition are firstly addressed. After that we introduce an EV-t algorithm for two-dimensional code acquisition. Then, the seven publications listed above are summarized. Finally, the asymptotic statistical properties of MUSIC are deeply analyzed in the special case that each user has two resolvable paths, and the analysis is based on the assumption that the space-time response vectors for a distinct set $\{\theta, \tau\}$ are linearly independent.

We conclude in Chapter 5 with a summary of the thesis and the direction of future work.

2 WIRELESS MOBILE COMMUNICATION CHANNEL

Compared to wireline channels, wireless channels present a greater challenge to communication system designers because of the propagation environment. The estimation and detection performances of the received signals are highly dependent upon the characteristics of the wireless channel. In some environments, perfect performance may be offered, whereas in other environments, a modest performance may be provided. Understanding the physical wireless propagation channels is essential to the development of good models for wireless signal processing. Before establishing a space-time array model, multipath propagation characteristics is first briefly introduced.

2.1 Multipath propagation characteristics

A signal propagated through an atmospheric medium can travel on multiple paths with different propagation delay, amplitude attenuation, and DOA etc., before they arrive at a receiver. In order to combat the versatile nature of the wireless channel, numerous efforts have been made to understand the underlying mechanism of wireless propagation.

2.1.1 Non-fading channel

The non-fading channel, called pass loss, is in particular a free-space channel which suffers only minor losses from atmospheric attenuation. It is a function of the distance between a transmitter and a receiver. Since there are no objects in the region to absorb or reflect energy, the power received by the receiver is given at [20]

$$p_r = p_t g_t g_r (\frac{\lambda}{4\pi \mathcal{D}})^2 \ , \tag{2}$$

where p_r is the received power, p_t is the transmitted power, g_r is the receive antenna's gain, g_t is the transmit antenna's gain, and $\mathcal{D}$ is the slant range between

the transmitter and the receiver. The wavelength (m) of the sinusoidal carrier signal is $\lambda = cf_c$, where the speed of light is $c = 3 \times 10^8$ m/s and f_c is the carrier frequency. From (2), we see that a free-space transmission formula depends on the inverse square of the separation distance $\mathcal{D}$.

Generally, a free-space line-of-sight (LOS) signal might not exist in a typical cellular environment. Instead, the receiver antenna experiences multipath signals for a single transmitted signal. When the signal is reflected by the plane earth surface, the vertical multipath causes more propagation attenuation, and the transmission loss over a plane earth is given by the approximation [20]

$$p_r = p_t g_t g_r (\frac{h_r h_t}{\mathcal{D}^2})^2 \ , \tag{3}$$

where h_r and h_t are the antenna height of the transmitter and the receiver. The received signal yields an $\mathcal{D}^4$ power relationship with the transmitter.

2.1.2 Fading channel

Fading can be roughly divided into two categories: fast fading and slow fading. Fast fading, also called small scale fading, is used to describe the rapid fluctuation of the amplitude of a radio signal over a short period of time. It is caused by the alternate constructive and destructive addition of multipath signals as a mobile terminal moves. There are two fast fading distributions. The first is Rayleigh fading which characterizes a multipath channel with non-line-of-sight (NLOS) situation. Using the baseband equivalent model [20], the gain of each multipath can be depicted as a complex gaussian random variable

$$h = h_x + jh_y \ , \tag{4}$$

where h_x and h_y are $N(0, \sigma_r^2)$ Gaussian random variables. The amplitude r_h and the phase θ_{r_h} of $h = r_h e^{j\theta_{r_h}}$ are given by

$$r_h = |h| = \sqrt{h_x^2 + h_y^2} \ , \tag{5}$$

$$\theta_{r_h} = tan^{-1}(\frac{h_x}{h_y}) \ . \tag{6}$$

Therefore, the expression of Rayleigh probability density function for r_h is given as [47]

$$f(r_h) = \frac{r_h}{\sigma_r^2} exp(-\frac{r_h^2}{2\sigma_r^2}) \ , \quad r_h \geq 0 \ . \tag{7}$$

The second typical type of fading model is Rician fading. Rician fading arises when there exists a line-of-sight (LOS) connection. Its probability density function is [47]

$$f(r_h) = \frac{r_h}{\sigma_r^2} \ exp(-\frac{r_h^2 + r_{h_0}^2}{2\sigma_r^2}) I_o(\frac{r_h r_{h_0}}{\sigma_r^2}) \ , \quad r_h \geq 0 \ , \tag{8}$$

where the constant r_{h_0} is the average power in the direct LOS, and $I_0(\cdot)$ is the modified Bessel function of the first kind and zero order [25]. We use κ to characterize the power in direct path to the power of non-direct paths, such that

$$\kappa = \frac{{r_{h_0}}^2}{2\sigma_r^2} \ . \tag{9}$$

Hence, the Rician probability density function can be further expressed as

$$f(r_h) = \frac{2\kappa r_h}{{r_{h_0}}^2} \ exp(-2\kappa(1 + r_h^2/{r_{h_0}}^2)) I_0(\frac{2\kappa r_h}{r_{h_0}}) \ , \quad r_{h_0} \geq 0 \ , \ r_h \geq 0 \ . \tag{10}$$

When $\kappa \rightarrow \infty$, the power of the dominant LOS signal is so strong. Hence, the channel does not exhibit fading. When $\kappa \rightarrow 0$, the line-of-sight signal disappears. The Rician density function tends to the Rayleigh density function.

The third model which can be used to model fast fading is Nakagami distribution which enables a better fit to experimental channel measurements. Its expression is given as [2]

$$f(r_h) = \frac{\varrho^\varrho r_h^{2\varrho-1}}{\Gamma(\varrho)\sigma_r^2} \ exp(-\frac{\varrho r_h^2}{2\sigma_r^2}) \ , \quad r_h \geq 0 \ , \tag{11}$$

where $\varrho = 4\sigma_r^4 / E\{(r_h^2 - 2\sigma_r^2)^2\}$ and $\Gamma(\cdot)$ is the gamma function. When the scattering process generates merely diffuse wave field, then $\varrho \approx 1$ and the Nakagami distribution is identical to the Rayleigh density function. When a direct LOS is present, the Nakagami distribution is approximate to the Rician density function as $\varrho > 1$.

Slow fading is also called large scale fading. It is caused by the shadowing effects of large buildings or natural features, and is determined by the local mean of a fast fading signal. The statistical distribution of the local mean has been studied experimentally. This distribution is influenced by the antenna heights, operating frequency, and the specific type of environment. However, it has been observed [31] that when all these parameters are fixed, the mean received power in a small neighborhood approaches a normal distribution when plotted on a logarithmic scale. Such a distribution is called log-normal and is described by the following probability density function

$$f(r_h) = \frac{1}{\sqrt{\pi}\sigma_r r_h} \ exp(-\frac{(log(r_h) - r_{hm})^2}{2\sigma_r^2}) \ , \quad r_h \geq 0 \ , \tag{12}$$

where r_{hm} is the mean of r_h.

2.1.3 Delay spread

In a multipath propagation environment, several time shifted versions of a transmitted signal arrive at a receiver. This results in the spreading of the signals in time. The spread of path delays is called delay spread. If the delay differences of all the multipath signals are very close to each other in the whole frequency

spectrum of the transmitted signal, the whole spectrum will behave similarly in the radio channel and flat fading is said to exist. Conversely, if the delay spread is comparable to or larger than the inverse of the bandwidth, the signal spectrum will be distorted and the fading will be frequency selective. Normally, the coherence of the bandwidth is related to the time delay spread, and can be expressed as [47] [49] [59]

$$C_{bd} = \varsigma \times \frac{1}{T_m} \ . \tag{13}$$

Here, ς is a multiplication constant and T_m is maximum excess delay. When the signal bandwidth is lower than the coherent bandwidth, the radio channel is called a narrowband channel. On the contrary, the radio channel is called a wideband channel.

2.1.4 Angle spread

The same as time delay spread, signal spreading can be described in DOA domain. Signal spreading in the DOA domain is described by the DOA power spectrum which assumes a finite number of propagation paths is discrete. However, as the receiver moves, the DOAs change, some paths disappear, new paths arise, and consequently the DOA spectrum also changes ultimately resulting in a continuous average spectrum.

2.1.5 Doppler shift

An important feature of mobile communication is that a transmitter communicates with a receiver while in motion. The velocity of the transmitter introduces a Doppler frequency shift and consequently generates carrier frequency spreading. The maximum Doppler frequency shift, f_D, is defined as [47] [49] [59]

$$f_D = \frac{\nu}{\lambda} \ , \tag{14}$$

where ν is the velocity(m/sec). When the moving vehicle with velocity ν transmits a continues-wave (CW) signal with carrier frequency f_c, the Doppler spectrum becomes

$$W(f) = \begin{cases} \frac{\sigma_r^2}{\pi\sqrt{f_D^2-(f-f_c)^2}} \ , & |f-f_c| \leq f_D \ , \\ 0 \ , & |f-f_c| > f_D \ , \end{cases} \tag{15}$$

where σ_r^2 is the average power of the signal.

The Doppler frequency shift f_D not only effects the Doppler spectrum but also determines the characteristics of fading. In the design of high speed digital mobile radio transmission systems, it is important to know the characteristics of multipath fading that induces burst errors. Provided that the burst errors occur when the signal envelope fades below a specific threshold value, the level crossing rate can be used as an appropriate measure for the burst error occurrence

rate. The fade duration may also be used to estimate the burst error length. The level crossing rate, which is generally defined as the expected rate at which the envelope R crosses a specified level R_s in the positive direction, is given by [27]

$$N_{R_s} = \sqrt{\pi} f_D \frac{R_s}{\sigma_r} \ exp(-\frac{R_s^2}{2\sigma_r^2}) \ . \tag{16}$$

The fade duration has also been shown at [27] to be

$$T_f = \frac{1}{\sqrt{\pi} f_D \frac{R_s}{\sigma_r}} \ exp(-\frac{R_s^2}{2\sigma_r^2} - 1) \ . \tag{17}$$

Hence, when the mobile velocity increases, the level cross rate R_s becomes larger and the fade duration T_f becomes smaller. In other words, the multipath fading varies faster.

Coherence time is defined as the required time interval to obtain an envelope correlation. It is inversely proportional to the maximum Doppler frequency, and is defined as [47] [49] [59]

$$C_T = \frac{1}{f_D} \ . \tag{18}$$

Coherence time provides us with an index of how fast the multipath fading varies. When we take two samples of a multipath signal at an interval larger than C_T, these two sample are slightly correlated. Hence, the smaller the coherent time is, the faster the channel varies.

2.2 Discrete space-time signal model

2.2.1 Information-bearing signal

The conducted data model is based on DS-CDMA wireless transmission systems. The kth user's transmitted baseband signal is given by

$$x_k(t) = \sum_{i=1}^{I} b_{k,i} s_k(t - iT) \tag{19}$$

under the consideration of binary phase-shift keying (BPSK) modulation, the kth user's transmitted symbol $b_{k,i} \in \{-1, 1\}$ for $i \in [1, I]$. T is one symbol duration. The spreading code $s_k(\cdot)$ assigned to kth user is modelled as

$$s_k(t) = \sum_{n=1}^{N} s_{k,n} \Pi(t - nT_c) \ , \tag{20}$$

where $s_{k,n} \in \{-1, +1\}$, $\Pi(t)$ denotes a unit rectangular pulse over the chip period T_c which is zero outside of $0 \leq t \leq T_c$. The integer $N = T/T_c$ is the processing gain.

Before transmitted, the baseband signal is uploaded on carrier frequency. As such, the transmitted signal is formed as

$$y_k(t) = \sqrt{P_k} x_k(t) e^{j(w_c t + \phi_k)} \ , \tag{21}$$

where P_k is the transmitted power of user k, w_c is the carrier frequency and ϕ_k is the random carrier phase uniformly distributed in $[0, 2\pi)$.

2.2.2 Antenna array

The antenna array is frequently used to receive the propagated signals. It can be arranged in various geometries, e.g. conformal array and plane array. Conformal array is that the elements of the antenna array are with a non-plane surface. Due to the simplicity of implementation, the plane array is the most commonly used structure. Linear array and circle array are two special cases of the planar array. Circle array means that the antenna elements lie in a circle. In the case of linear array, the antenna elements are aligned along with a straight line. With equal spacing, the linear array is called uniform linear array. In this thesis, a uniform linear array is used.

Figure 1 illustrates a M-element uniform linear array spaced with a distance d_u. For analyzing the uniform linear array, a reference point is established in this figure. With the assumption that the transmitted signals originated far away from the array, the directions of propagation paths are approximately the same at each element. Hence, the array response vector corresponding to the direction θ can be expressed as

$$\mathbf{a}(\theta) = \begin{pmatrix} \mathrm{a}^1(\theta) \\ \mathrm{a}^2(\theta) \\ \vdots \\ \mathrm{a}^M(\theta) \end{pmatrix} . \tag{22}$$

A standard narrowband assumption typically used in array signal processing is made here. In this case the signal bandwidth is small compared to the carrier frequency, and the time delay due to physical array only causes a phase shift on the impinging signal. If the propagation distance from the first element to the second element is $d_u \sin(\theta)$, the propagation time due to the propagation distance is given as $d_u sin(\theta)/c$. Hence, the effect of propagation time on the signal has a phase shift $e^{j2\pi f_c \tau_u}$, where $\tau_u = d_u sin(\theta)/c$. From the first element to mth element, the phase shift can be expressed as $e^{j2\pi f_c (m-1) d_u sin(\theta)/c}$ and the array response vector (22) can be re-written as

$$\mathbf{a}(\theta) = \begin{pmatrix} 1 \\ e^{j2\pi f_c \frac{d_u \sin(\theta)}{c}} \\ \vdots \\ e^{j2\pi f_c (M-1) \frac{d_u \sin(\theta)}{c}} \end{pmatrix} . \tag{23}$$

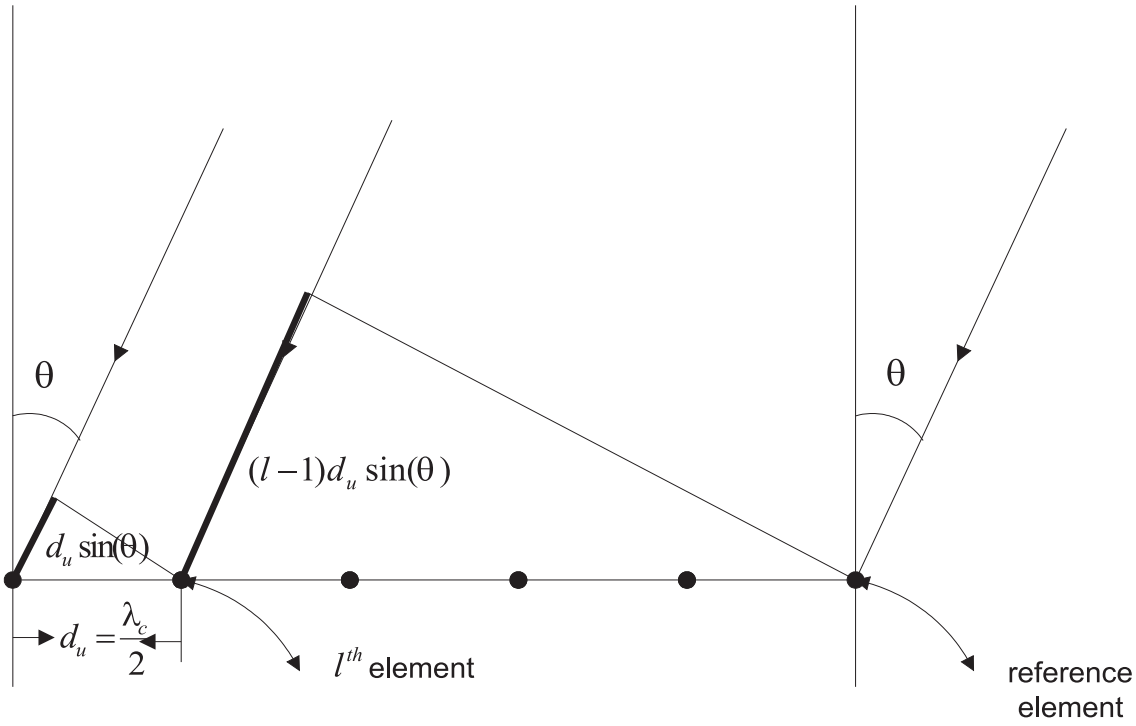

FIGURE 1 An M-elements uniform linear array (ULA) with inter-sensor spacing d_u.

Spatial aliasing and mutual coupling are two important factors of inter-element spacing. To avoid spatial aliasing, the element spacing of an array should always be less than or equal to half of the carrier wavelength λ, which is given as $\frac{c}{f_c}$. However, the element spacing can not be made arbitrarily small since two close spaced antenna elements exhibit a mutual coupling effect. This mutual coupling is caused by mutual impedance [70] defined as the voltage induced on one element by a current in the other element. Mutual impedance is present over a broad range of element spacing d_u, however for $d_u < \frac{\lambda}{2}$ the mutual impedance tends to increase considerably.

To avoid the spatial aliasing and the mutual coupling effects, the equal spacing $d_u = \frac{\lambda}{2}$ is devised among antenna elements in practice, and the array response vector can be finally given as

$$\mathbf{a}(\theta) = \begin{pmatrix} 1 \\ e^{j\pi \sin(\theta)} \\ \vdots \\ e^{j(M-1)\pi \sin(\theta)} \end{pmatrix}. \tag{24}$$

In general, the array response vector is a function of the individual element response, the array geometry, and signal frequency. Here it is only a function of DOA.

2.2.3 The space-time manifold

A uniform linear array with M elements is used to receive the transmitted signals. The expression of received signals into mth element is

$$r^{m'}(t) = \sum_{k=1}^{K}\sum_{l=1}^{L}\sqrt{P_{k,l}}x_k(t-\tau_{k,l})e^{j(w_c t+\phi_k^{'})}e^{j(m-1)\pi\sin(\theta_{k,l})}+n^{m'}(t) \ , \quad (25)$$

where $\phi_k^{'} = \phi_k - w_c\tau_{k,l}$ and $n^{m'(t)}$ is noise. After down-conversion the received signals at the mth element can be expressed as

$$r^{m}(t) = \sum_{k=1}^{K}\sum_{l=1}^{L}a_{k,l}x_k(t-\tau_{k,l})e^{j(m-1)\pi\sin(\theta_{k,l})}+n^{m}(t) \ , \quad (26)$$

where the contribution of $\sqrt{P_{k,l}}e^{j(\phi_k - w_c\tau_{k,l})}$ is included in $a_{k,l}$. With a fast moving transmitter, the channel characteristics change rapidly over time. We assume that the varying channel is approximately constant over the time span of one symbol, but varies symbol to symbol. In this situation, the corresponding received signal during symbol i at the mth element is rewritten as

$$r^{m}(t) = \sum_{k=1}^{K}\sum_{l=1}^{L}a_{k,l,i}x_k(t-\tau_{k,l})e^{j(m-1)\pi\sin(\theta_{k,l})}+n^{m}(t) \ . \quad (27)$$

We call $a_{k,l,i}$ as attenuation factor. Variables $\tau_{k,l}$ and $\theta_{k,l}$ are time delay and DOA, respectively. They are assumed to remain roughly constant within the observation interval. In front of each element, a chip-MF is equipped to convert a continuous-time signal to a discrete-time signal and perform integrate and dump operation. After sampling, the output of the complex received signals $r^m(t)$ in a chip interval may be written as

$$\frac{1}{T_c}\int_{nT_c}^{(n+1)T_c} r^m(t)dt \ . \quad (28)$$

Due to asynchronous transmission, we enlarge the observation window to the size of two symbols for getting one whole transmitted symbol within the window. Thus, the sampled data vector for symbol i is

$$\mathbf{r}_i^m = [r^m[iN+1], r^m[iN+2], ..., r^m[(i+2)N]] \ , \quad (29)$$

which can be described as

$$\begin{aligned}\mathbf{r}_i^m &= \sum_{k=1}^{K}\sum_{l=1}^{L}[b_{k,i-1}a_{k,l,i-1}\underline{\mathbf{c}}_{k,l}e^{j(m-1)\pi\sin(\theta_{k,l})}+b_{k,i}a_{k,l,i}\mathbf{c}_{k,l}e^{j(m-1)\pi\sin(\theta_{k,l})} \quad (30)\\ &+ b_{k,i+1}a_{k,l,i+1}\bar{\mathbf{c}}_{k,l}e^{j(m-1)\pi\sin(\theta_{k,l})}]+\mathbf{n}_i^m \ .\end{aligned}$$

Here

$$\begin{aligned}\underline{\mathbf{c}}_{k,l} &= \underline{\mathbf{c}}_{k,l}(\tau_{k,l}) = (1-\zeta_{k,l})\underline{\mathbf{g}}_{k,l}(h_{k,l})+\zeta_{k,l}\underline{\mathbf{g}}_{k,l}(h_{k,l}+1) \ ,\\ \mathbf{c}_{k,l} &= \mathbf{c}_{k,l}(\tau_{k,l}) = (1-\zeta_{k,l})\mathbf{g}_{k,l}(h_{k,l})+\zeta_{k,l}\mathbf{g}_{k,l}(h_{k,l}+1) \ ,\\ \bar{\mathbf{c}}_{k,l} &= \bar{\mathbf{c}}_{k,l}(\tau_{k,l}) = (1-\zeta_{k,l})\bar{\mathbf{g}}_{k,l}(h_{k,l})+\zeta_{k,l}\bar{\mathbf{g}}_{k,l}(h_{k,l}+1) \ .\end{aligned}$$

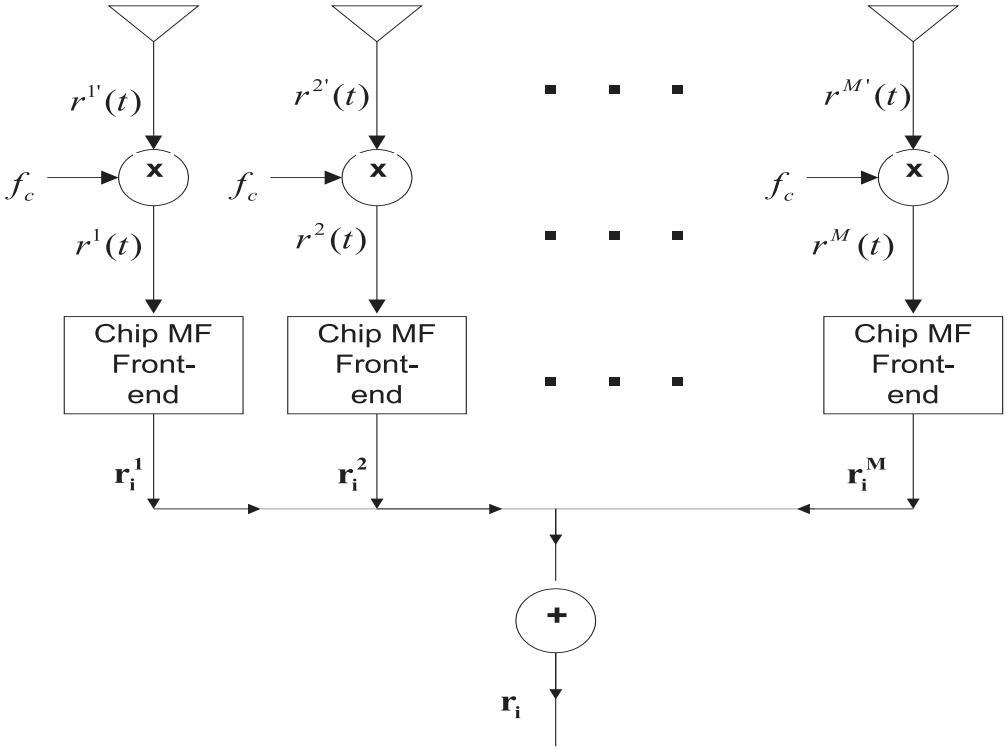

FIGURE 2 Structure of receiver with an uniform linear array

The "previous", "current", and the "next" code vectors can be written, respectively, as

$$\begin{aligned}
\underline{\mathbf{g}}_{k,l} &= \underline{\mathbf{g}}_{k,l}(h_{k,l}) = [s_{k,N-h_{k,l}+1}, ..., s_{k,N}, \overbrace{0, \ldots, 0}^{2N-h_{k,l}}]^T \ , \\
\mathbf{g}_{k,l} &= \mathbf{g}_{k,l}(h_{k,l}) = [0, \ldots, 0, s_{k,1}, \ldots, s_{k,N}, 0, \ldots, 0]^T \ , \\
\overline{\mathbf{g}}_{k,l} &= \overline{\mathbf{g}}_{k,l}(h_{k,l}) = [\underbrace{0, \ldots, 0}_{N+h_{k,l}}, s_{k,1}, \ldots, s_{k,N-h_{k,l}}]^T \ .
\end{aligned}$$

The exact time delay of kth user's lth path can be expressed as $\tau_{k,l} = h_{k,l}T_c + \zeta_{k,l}$, where $h_{k,l}$ and $\zeta_{k,l}$ are the integer and fractional part of time delay $\tau_{k,l}$ respectively.

The overall sampled signals at the antenna array can be compactly expressed as

$$\begin{aligned}
\mathbf{r}_i &= \sum_{k=1}^{K}\sum_{l=1}^{L} [b_{k,i-1}a_{k,l,i-1}\underline{\mathbf{c}}_{k,l} \otimes \mathbf{a}_{k,l} + b_{k,i}a_{k,l,i}\mathbf{c}_{k,l} \otimes \mathbf{a}_{k,l} \\
&+ b_{k,i+1}a_{k,l,i+1}\overline{\mathbf{c}}_{k,l} \otimes \mathbf{a}_{k,l}] + \mathbf{n}_i \quad ,
\end{aligned} \tag{31}$$

where $\mathbf{a}_{k,l} = \mathbf{a}_{k,l}(\theta_{k,l}) = [1, e^{j\pi\sin(\theta_{k,l})}, \ldots, e^{j(M-1)\pi\sin(\theta_{k,l})}]^T$, and $(\cdot)^T$ denotes the transpose operation. Similarly to the array response vectors $\mathbf{a}_{k,l}$, the space-time response vectors are defined as

$$\underline{\mathbf{h}}_{k,l} = \underline{\mathbf{h}}_{k,l}(\theta,\tau) = \underline{\mathbf{c}}_{k,l} \otimes \mathbf{a}_{k,l} \ , \tag{32}$$

$$\mathbf{h}_{k,l} = \mathbf{h}_{k,l}(\theta,\tau) = \mathbf{c}_{k,l} \otimes \mathbf{a}_{k,l} \ , \tag{33}$$

$$\overline{\mathbf{h}}_{k,l} = \overline{\mathbf{h}}_{k,l}(\theta,\tau) = \overline{\mathbf{c}}_{k,l} \otimes \mathbf{a}_{k,l} \ , \tag{34}$$

where $\otimes$ denotes the kronecker product. Finally, the compact representation of (31) can be expressed as

$$\mathbf{r}_i = \mathbf{H}\mathbf{A}_i\mathbf{b}_i + \mathbf{n}_i = \mathbf{H}\mathbf{f}_i + \mathbf{n}_i \ . \tag{35}$$

The $2MN \times 3KL$ matrix $\mathbf{H} = [\underline{\mathbf{h}}_{1,1}, \mathbf{h}_{1,1}, \overline{\mathbf{h}}_{1,1}, ..., \underline{\mathbf{h}}_{K,L}, \mathbf{h}_{K,L}, \overline{\mathbf{h}}_{K,L}]$. The dimension of $\mathbf{A}_i$ corresponding to ith sampled symbol is $3KL \times 3K$. Its expression is $\mathbf{A}_i = diag\{\mathbf{A}_{1,i}, ..., \mathbf{A}_{k,i}, ...\mathbf{A}_{K,i}\}$, and

$$\mathbf{A}_{k,i} = \begin{pmatrix} a_{k,1,i-1} & 0 & 0 \\ 0 & a_{k,1,i} & 0 \\ 0 & 0 & a_{k,1,i+1} \\ \vdots & \vdots & \vdots \\ a_{k,L,i-1} & 0 & 0 \\ 0 & a_{k,L,i} & 0 \\ 0 & 0 & a_{k,L,i+1} \end{pmatrix} . \tag{36}$$

Finally, $\mathbf{b}_i = [b_{1,i-1}, b_{1,i}, b_{1,i+1}, \ldots, b_{K,i-1}, b_{K,i}, b_{K,i+1}]^T$, and $\mathbf{f}_i = [f_{1,1,i-1}, f_{1,1,i}, f_{1,1,i+1}, \cdots, f_{K,L,i-1}, f_{K,L,i}, f_{K,L,i+1}]^T$, where $f_{k,l,i-1} = a_{k,l,i-1}b_{k,i-1}$, $f_{k,l,i} = a_{k,l,i}b_{k,i}$, and $f_{k,l,i+1} = a_{k,l,i+1}b_{k,i+1}$.

With I symbol collection, (35) has the form as

$$\mathbf{R} = \mathbf{H}\mathbf{F} + \mathbf{N} \ , \tag{37}$$

where $\mathbf{F} = [\mathbf{f}_1, ..., \mathbf{f}_I]$, and $\mathbf{N} = [\mathbf{n}_1, ..., \mathbf{n}_I]$.

2.2.4 Basic assumptions

The common assumptions are made as follows:

As1. Under the consideration of BPSK modulation, symbols in vector $\mathbf{b}_i$ are assumed random and independent binary variables with zero mean, e.g. $E\{b_{k,i}\} = 0$, and $E\{b_{k,i}b_{p,j}\} = 0$ if $k \neq p$ and/or $i \neq j$, where $E\{\cdot\}$ is the expectation operator.

As2. The correlation coefficient between the various paths from the same user is defined as $\rho_{k(l,l')} = E\{a_{k,l,i}a^*_{k,l',i}\}/E\{||a_{k,l,i}||\}E\{||a^*_{k,l',i}||\}$, where $||\cdot||$ stands for the norm, and $(\cdot)^*$ denotes the complex conjugate. We assume symbol variables are uncorrelated with attenuations factors.

As3. The additive noise variables in the vector $\mathbf{n}_i$ are temporally and spatially complex circular white gaussian random variables with zero mean. Owing to circularity of $\mathbf{n}_i$, we have $E\{\mathbf{n}_i\mathbf{n}_j^T\} = \mathbf{0}_{2MN\times 2MN}$ and $E\{\mathbf{n}_i\mathbf{n}_j^H\} = \sigma^2\mathbf{I}_{2MN}\delta_{i,j}$. $(\cdot)^H$ denotes complex conjugate transpose, $\mathbf{I}$ is the $2NM \times 2NM$ identify matrix, and $\delta_{i,j}$ denotes the kronecker delta. The additive noise variables are uncorrelated with symbol variables in vector $\mathbf{b}_i$ and attenuations factors in matrix $\mathbf{A}_i$.

As4. The number of incident signals is assumed to be known, and the necessary conditions $3KL < 2MN$ and $3KL < I$ are required.

Remark: These conditions maintain $\mathbf{r}_i$ to be a rank deficient matrix, in which guarantee a unique identifiability of $\{\theta, \tau\}$. $3KL < 2MN$ is required as a necessary condition to keep $\mathbf{H}$ strictly tall and full column rank. Meanwhile, the matrix $\mathbf{F}$ must be full row rank: this implies $3KL < I$.

3 OVERVIEW OF SPACE-TIME PARAMETER ESTIMATION

Parameter estimation is a pre-requisite task for obtaining the transmitted symbols. This chapter gives a view of the class of algorithms for parameter estimation, especially for two-dimensional code acquisition.

3.1 Conventional parameter estimation methods

The standard beamformer and capon's minimum variance method [8] [66] are classified as conventional parameter estimation methods. With the assumption that the first user is of interest, the standard beamformer for DOA estimation in the space array model is defined as

$$\mathbf{w}_{BF} = \frac{\hat{\mathbf{a}}(\theta)}{\sqrt{\hat{\mathbf{a}}^H(\theta)\hat{\mathbf{a}}(\theta)}} \quad . \tag{38}$$

Capon's minimum variance method attempts to minimize the total output power while maintaining a constant gain in the desired direction. Its weight vector is

$$\mathbf{w}_{CAP} = \frac{\mathbf{R}_r^{-1}\hat{\mathbf{a}}(\theta)}{\hat{\mathbf{a}}^H(\theta)\mathbf{R}_r^{-1}\hat{\mathbf{a}}(\theta)} \quad . \tag{39}$$

In practice, the ensemble correlation matrix $\mathbf{R}_r$ is replaced by the sample correlation matrix $\hat{\mathbf{R}}_r$, where $\hat{\mathbf{R}}_r = \frac{1}{I}\sum_{i=1}^{I} \mathbf{r}_i\mathbf{r}_i^H$.

The above weight vectors behave as spatial filters, and they can be used for two-dimensional cod acquisition as follows.

3.1.1 Standard beamformer for two-dimensional code acquisition

For two-dimensional code acquisition, the weight vector of the standard beamformer can be imitated as

$$\mathbf{w}_{ST-BF} = \frac{\hat{\mathbf{h}}_{1,l}}{\sqrt{\hat{\mathbf{h}}_{1,l}^H \hat{\mathbf{h}}_{1,l}}} \ , \tag{40}$$

where $\hat{\mathbf{h}}_{1,l} = \mathbf{c}_{1,l} \otimes \mathbf{a}_{1,l}$ is the space-time response vector for the first user's lth path, see section 2.2.3. The two-dimensional code acquisition can then be performed according to

$$\begin{aligned} \{\hat{\tau}_{1,1}, \hat{\theta}_{1,1}, \cdots, \hat{\tau}_{1,L}, \hat{\theta}_{1,L}\} &= argmax_{\boldsymbol{\tau},\boldsymbol{\theta}} \ \mathbf{w}_{ST-BF}^H \hat{\mathbf{R}}_r \mathbf{w}_{ST-BF} \\ &= argmax_{\boldsymbol{\tau},\boldsymbol{\theta}} \ \frac{\hat{\mathbf{h}}_{1,l}^H \hat{\mathbf{R}}_r \hat{\mathbf{h}}_{1,l}}{\hat{\mathbf{h}}_{1,l}^H \hat{\mathbf{h}}_{1,l}} \ . \end{aligned} \tag{41}$$

In general, the L highest peaks on the two-dimensional spectrum should be chosen, and there is only one peak corresponding to one pair of DOA and time delay. However, the practical system exhibits strong non-idealities which leads to relatively wide main-lobes for the standard beamformer. Its solution is not sharp, and the limited effectiveness is caused by the power from close adjacent signals [16].

3.1.2 Capon's minimum variance method for two-dimensional code acquisition

This method minimizes the contributions of the signals along the undesired DOA and time delay, while maintaining a constant gain in the desired space-time direction. The constrained minimization problem can be given mathematically as

$$\begin{aligned} \mathbf{w}_{ST-CAP} = argmin_{\boldsymbol{\tau},\boldsymbol{\theta}} \ \mathbf{w}_{ST-BF}^H \hat{\mathbf{R}}_r \mathbf{w}_{ST-BF} \\ \text{subject to} \qquad |\mathbf{w}_{ST-BF}^H \hat{\mathbf{h}}_{1,l}| = 1 \ . \end{aligned} \tag{42}$$

The solution to the above problem is [16]

$$\mathbf{w}_{ST-CAP} = \frac{\hat{\mathbf{R}}_r^{-1} \hat{\mathbf{h}}_{1,l}}{\hat{\mathbf{h}}_{1,l}^H \hat{\mathbf{R}}_r^{-1} \hat{\mathbf{h}}_{1,l}} \ . \tag{43}$$

Equation (43) is called a minimum variance distortionless response (MVDR) beamformer weight vector. Using the weight vector, the two-dimensional code acquisition can be obtained by

$$\begin{aligned} \{\hat{\tau}_{1,1}, \hat{\theta}_{1,1}, \cdots, \hat{\tau}_{1,L}, \hat{\theta}_{1,L}\} &= argmax_{\boldsymbol{\tau},\boldsymbol{\theta}} \ \mathbf{w}_{ST-CAP}^H \hat{\mathbf{R}}_r \mathbf{w}_{ST-CAP} \\ &= argmax_{\boldsymbol{\tau},\boldsymbol{\theta}} \ \frac{1}{\hat{\mathbf{h}}_{1,l}^H \hat{\mathbf{R}}_r^{-1} \hat{\mathbf{h}}_{1,l}} \ . \end{aligned} \tag{44}$$

3.2 Maximum likelihood methods

The modern history of the maximum likelihood (ML) method starts from the work of R. A. Fisher [13]. In a maximum likelihood estimation, the estimator is chosen such that the likelihood is maximized by selecting a set of parameters that make the observed data most probable. Two methods [37] called stochastic maximum likelihood (SML) and deterministic maximum likelihood (DML) are widely studied. For SML technique, $\mathbf{s}(t)$ and $\mathbf{n}(t)$ in the space array model are modelled as gaussian. On the other hand, $\mathbf{s}(t)$ in DML is modelled as unknown deterministic quantities, and $\mathbf{n}(t)$ is gaussian. Correspondingly, the names of a conditional and unconditional ML method are given for SML and DML in [64].

As the parameter estimation problem is considered in DS-CDMA systems, DML method is exploited in [69] and [80]. In the following only DML is addressed for two-dimensional code acquisition.

3.2.1 Deterministic maximum likelihood

The DML method was at first called the classical ML method in [24], since the model contains unknown deterministic parameters. Its consistency and asymptotic distribution are considered in [33] [34] [36] [77] [78], and the consistency and asymptotic covariance are considered in [62] [63].

[69] proposes DML method for time delay estimation in DS-CDMA systems. [80] explores the DML method for two-dimensional code acquisition in DS-CDMA arrays, where a time non-varying channel model is assumed. This means that the attenuation factors of (35) are fixed for the observation interval. In this case, we use $\mathbf{A}$ to replace $\mathbf{A}_i$ below. Using DML for two-dimensional code acquisition, the received data $\mathbf{r}_i$ are modelled and parameterized by $\boldsymbol{\tau}$, $\boldsymbol{\theta}$, $\mathbf{A}$ with a mean vector

$$E\{\mathbf{r}_i\} = \mathbf{HAb}_i \tag{45}$$

and the second moment matrices

$$\begin{aligned} E\{(\mathbf{r}_i - E\{\mathbf{r}_i\})(\mathbf{r}_j - E\{\mathbf{r}_j\})^H\} &= \mathbf{Q}\delta_{i,j} \ , \\ E\{(\mathbf{r}_i - E\{\mathbf{r}_i\})(\mathbf{r}_j - E\{\mathbf{r}_j\})^T\} &= \mathbf{0} \ , \end{aligned} \tag{46}$$

where $\delta_{i,j}$ is a discrete kronecker delta function, and $\mathbf{Q}$ is the covariance matrix for the white noise vector $\mathbf{n}_i$, e.g. $\mathbf{Q} = \mathbf{I}_{2MN}$. The likelihood function for $\mathbf{r}_i$ is given as

$$L\{\mathbf{r}_i; \boldsymbol{\tau}, \boldsymbol{\theta}, \mathbf{A}, \mathbf{Q}\} = \frac{1}{\pi^{2NM}|\mathbf{Q}|} \ exp\{-\mathbf{n}_i^H \mathbf{Q}^{-1} \mathbf{n}_i\} \ , \tag{47}$$

here $|\cdot|$ stands for the determinant, and $\mathbf{n}_i$ is given as

$$\mathbf{n}_i = \mathbf{r}_i - \mathbf{HAb}_i \ . \tag{48}$$

Because $\mathbf{r}_i$ and $\mathbf{r}_j$ are uncorrelated for $i \neq j$, the likelihood function for $\mathbf{R} = [\mathbf{r}_1, \ldots, \mathbf{r}_I]$ can be written as

$$L\{\mathbf{R}; \boldsymbol{\tau}, \boldsymbol{\theta}, \mathbf{A}, \mathbf{Q}\} = \prod_{i=1}^{I} L\{\mathbf{r}_i; \boldsymbol{\tau}, \boldsymbol{\theta}, \mathbf{A}, \mathbf{Q}\} = \frac{1}{\pi^{2NMI}|\mathbf{Q}|^I} \; exp\{-\sum_{i=1}^{I} \mathbf{n}_i^H \mathbf{Q}^{-1} \mathbf{n}_i\} \; . \quad (49)$$

The log likelihood function has the following form [69]

$$l\{\boldsymbol{\tau}, \boldsymbol{\theta}, \mathbf{A}, \mathbf{Q}\} = -I \; log(|\mathbf{Q}|) - Tr\{\mathbf{Q}^{-1}\mathbf{e}(\boldsymbol{\theta}, \boldsymbol{\tau}, \mathbf{A})\} \; , \quad (50)$$

where

$$\mathbf{e}(\boldsymbol{\theta}, \boldsymbol{\tau}, \mathbf{A}) = \frac{1}{I} \sum_{i=1}^{I} (\mathbf{r}_i - \mathbf{HAb}_i)(\mathbf{r}_i - \mathbf{HAb}_i)^H \; . \quad (51)$$

Since the natural logarithm is a strictly increasing function of its argument, it is all the same to maximize the log-likelihood function as to maximize the likelihood function itself. If the log-likelihood function is derived with respect to unknown parameters (DOA, time delay, attenuation factor, and $\mathbf{Q}$), the derivative is set to equal zero. The parameter estimation function is therefore equally given as

$$\{\hat{\boldsymbol{\tau}}, \hat{\boldsymbol{\theta}}, \hat{\mathbf{A}}, \hat{\mathbf{Q}}\} = argmax_{\boldsymbol{\tau}, \boldsymbol{\theta}, \mathbf{A}, \mathbf{Q}} \; l\{\boldsymbol{\tau}, \boldsymbol{\theta}, \mathbf{A}, \mathbf{Q}\} \; . \quad (52)$$

The negative log-likelihood function is minimized with respect to $\mathbf{Q}$ by

$$|\hat{\mathbf{Q}}| = \mathbf{e}(\boldsymbol{\theta}, \boldsymbol{\tau}, \mathbf{A}) \; . \quad (53)$$

It now remains to minimize

$$l\{\boldsymbol{\theta}, \boldsymbol{\tau}, \hat{\mathbf{Q}}, \mathbf{A}\} = log|\mathbf{e}(\boldsymbol{\theta}, \boldsymbol{\tau}, \mathbf{A})| + constant \; . \quad (54)$$

After some manipulations, it can be shown that the DML estimate of $\mathbf{A}$ equals [69]

$$\hat{\mathbf{A}} = \hat{\mathbf{R}}_{bb}^{-1} \hat{\mathbf{R}}_{rb}^H \hat{\mathbf{W}}^{-1} \mathbf{H} (\mathbf{H}^H \hat{\mathbf{W}^{-1}} \mathbf{H})^{-1} \; , \quad (55)$$

where

$$\hat{\mathbf{R}}_{bb} = \frac{1}{I} \sum_{i=1}^{I} \mathbf{b}_i \mathbf{b}_i^T \; , \quad (56)$$

$$\hat{\mathbf{R}}_{rb} = \frac{1}{I} \sum_{i=1}^{I} \mathbf{r}_i \mathbf{b}_i^T \; , \quad (57)$$

$$\hat{\mathbf{W}} = \hat{\mathbf{R}}_r - \hat{\mathbf{R}}_{rb} \hat{\mathbf{R}}_{bb}^{-1} \hat{\mathbf{R}}_{rb}^H \; , \quad (58)$$

$$\hat{\mathbf{R}}_r = \frac{1}{I} \sum_{i=1}^{I} \mathbf{r}_i \mathbf{r}_i^H \; . \quad (59)$$

For sufficiently large I, the assumption that $\hat{\mathbf{W}}$ is invertible is true. As $I \rightarrow \infty$, $\hat{\mathbf{W}}$ approach to $\mathbf{Q}$ with probability one.

Hence, the two-dimensional code acquisition can be given as

$$\{\hat{\boldsymbol{\theta}}, \hat{\boldsymbol{\tau}}\} = argmin_{\boldsymbol{\tau},\boldsymbol{\theta}}\, log\, |\mathbf{I} - \hat{\mathbf{R}}_{bb}^{-\frac{1}{2}} \hat{\mathbf{R}}_{rb}^{H} \hat{\mathbf{W}}^{-\frac{1}{2}} \mathbf{X} \hat{\mathbf{W}}^{-\frac{1}{2}} \hat{\mathbf{R}}_{rb} \hat{\mathbf{R}}_{bb}^{-\frac{1}{2}}| \ , \tag{60}$$

where $\mathbf{X} = \mathbf{I} - \hat{\mathbf{W}}^{-\frac{1}{2}} \mathbf{H} (\mathbf{H}^H \hat{\mathbf{W}}^{-1} \mathbf{H})^{-1} \mathbf{H}^H \hat{\mathbf{W}}^{-\frac{1}{2}}$. Wax [82] was the first one to propose DML method for two-dimensional code acquisition. In [82], the DML method for two-dimensional code acquisition was developed for one user system over AWGN channels. As DML method was considered for DS-CDMA systems, [80] exploited the single user DML estimator. This means that undesired users are seen as noise. The advantage of the approach is that the search is processed on one user's space. The price to pay for the saved computation is that some performance is likely to be lost.

3.3 Subspace methods

Subspace based methods exploit the structure of received data model. They are frequently considered as powerful techniques for parameter estimation. Examples of typical subspace based methods include multiple signal classification (MUSIC) [60], root-MUSIC [5], estimation of signal parameters via rotational invariance techniques (ESPRIT) [58], minimum norm (Min-Norm) [26] [50] , method of direction estimation (MODE) [65], weight subspace fitting (WSF) [37] [78] [79], and eigenvector (EV) estimator [21] etc.

The basic idea of subspace based methods is that the sample auto-correlation matrix needs to be divided into the signal and noise subspaces. Since the desired signal is within the signal subspace, the parameter estimation is performed by seeking the orthogonality between the noise subspace and the signal of interest. Based on assumption *As1*, *As3*, and equation (35), the ensemble correlation matrix of vector $\mathbf{r}_i$ can be written as

$$\mathbf{R}_r \ = \ E\{\mathbf{r}_i \mathbf{r}_i^H\} = E\{(\mathbf{H}\mathbf{f}_i + \mathbf{n}_i)(\mathbf{H}\mathbf{f}_i + \mathbf{n})_i^H\} = \mathbf{H}\mathbf{R}_{f(i)}\mathbf{H}^H + \sigma^2\mathbf{I} \ , \tag{61}$$

Regarding the assumptions *As1* and *As2*, the correlation matrix of $\mathbf{f}_i$ is

$$\mathbf{R}_{f(i)} \ = \ E\{\mathbf{f}_i \mathbf{f}_i^H\} = E\{\mathbf{A}_i \mathbf{A}_i^H\} = \mathbf{R}_{A(i)} \ , \tag{62}$$

where

$$\mathbf{R}_{A(i)} = diag\{\mathbf{R}_{A(1,i)}, ..., \mathbf{R}_{A(k,i)}, ...\mathbf{R}_{A(K,i)}\} \ . \tag{63}$$

$\mathbf{R}_{A(k,i)}$ is shown at the top of this page, and $a'_{k,(l,l'),i-1} = E\{a_{k,l,i-1} a^*_{k,l',i-1}\}$, $a'_{k,(l,l'),i} = E\{a_{k,l,i} a^*_{k,l',i}\}$, $a'_{k,(l,l'),i+1} = E\{a_{k,l,i+1} a^*_{k,l',i+1}\}$. Due to the high-correlation/coherency between the various paths, $\mathbf{R}_{f(i)} = \mathbf{R}_{A(i)}$ has a rank reduction.

$$\mathbf{R}_{A(k,i)} = \tag{64}$$

$$\begin{pmatrix}
a'_{k,(1,1),i-1} & 0 & 0 & \dots & a'_{k,(1,L),i-1} & 0 & 0 \\
0 & a'_{k,(1,1),i} & 0 & \dots & 0 & a'_{k,(1,L),i} & 0 \\
0 & 0 & a'_{k,(1,1),i+1} & \dots & 0 & 0 & a'_{k,(1,L),i+1} \\
\vdots & \vdots & \vdots & \vdots & \vdots & \vdots & \vdots \\
a'_{k,(L,1),i-1} & 0 & 0 & \dots & a'_{k,(L,L),i-1} & 0 & 0 \\
0 & a'_{k,(L,1),i} & 0 & \dots & 0 & a'_{k,(L,L),i} & 0 \\
0 & 0 & a'_{k,(L,1),i+1} & \dots & 0 & 0 & a'_{k,(L,L),i+1}
\end{pmatrix} .$$

The ensemble correlation matrix $\mathbf{R}_r$ (61) can be eigen-decomposed as

$$\mathbf{R}_r = \mathbf{U}\mathbf{\Lambda}\mathbf{U}^H = \mathbf{U}_s\mathbf{\Lambda}_s\mathbf{U}_s^H + \mathbf{U}_n\mathbf{\Lambda}_n\mathbf{U}_n^H \ , \tag{65}$$

where $\mathbf{\Lambda}_s$ contains the eigenvalues of the signal subspace in descending order, and can be expressed as

$$\mathbf{\Lambda}_s = diag\{\lambda_1, \cdots, \lambda_D\} \ , \tag{66}$$

where D is the dimension of the signal subspace. $\mathbf{U}_s$ contains the corresponding eigenvectors. Practically, the ensemble correlation matrix $\mathbf{R}_r$ is not available, and a sample correlation matrix $\hat{\mathbf{R}}_r$ is used instead and eigen-decomposed into

$$\hat{\mathbf{R}}_r = \frac{1}{I}\sum_{i=1}^{I}\mathbf{r}_i\mathbf{r}_i^H = \hat{\mathbf{U}}\hat{\mathbf{\Lambda}}\hat{\mathbf{U}}^H = \hat{\mathbf{U}}_s\hat{\mathbf{\Lambda}}_s\hat{\mathbf{U}}_s^H + \hat{\mathbf{U}}_n\hat{\mathbf{\Lambda}}_n\hat{\mathbf{U}}_n^H \ , \tag{67}$$

where $\hat{\mathbf{\Lambda}}_s$ contains the estimated eigenvalues of the signal subspace, correspondingly $\hat{\mathbf{U}}_s$ contains the estimated eigenvectors of the signal subspace.

In the following, the two most common subspace methods, MUSIC and ESPRIT, are addressed for two-dimensional code acquisition.

3.3.1 MUSIC

MUSIC is a blind estimator which was originally proposed in [60] for DOA estimation. In addition to the DOA estimation, [6] [67] [68] use MUSIC for time delay estimation. Due to several essential benefits, some literature, e.g. [48] [81], use MUSIC for two-dimensional code acquisition. In [81], the combination of one spatial MUSIC for DOA estimation and two temporal MUSIC for time delay

estimation is used for two-dimensional code acquisition. Further, MUSIC ís presented in [48] for two-dimensional code acquisition, and the conditional CRLB is derived. [15] [17] [29] use MUSIC for two-dimensional code acquisition in the DS-CDMA data model. [15] simply employs MUSIC for two-dimensional code acquisition in an asynchronous DS-CDMA system with a fast fading multipath channel. In [17] a pre-processing operation, temporal and spatial smoothing, is proposed before using MUSIC for the two-dimensional code acquisition. In [29], a code-reuse technique is used. Due to the approach of a space-time preprocessor to code-reuse, undesired signals are removed before MUSIC performs the two-dimensional code acquisition.

The original MUSIC method is formulated for the case that each column of $\mathbf{A}(\theta)$ in the space array model (1) is parameterized by distinct values θ. For two-dimensional code acquisition, MUSIC can be established by the fact that the desired user's space-time response vector at the correct timing and angle offset must be orthogonal to the noise subspace. Below, two steps describe the MUSIC method to perform two-dimensional code acquisition.

1. Eigen-decomposes the sample correlation matrix $\hat{\mathbf{R}}_r$ to form the mutually orthogonal signal subspace and noise subspace as

$$\hat{\mathbf{R}}_r = \hat{\mathbf{U}}_s \hat{\mathbf{\Lambda}}_s \hat{\mathbf{U}}_s^H + \hat{\mathbf{U}}_n \hat{\mathbf{\Lambda}}_n \hat{\mathbf{U}}_n^H \ . \tag{68}$$

2. Performs parameter estimation by intersecting a replica of the desired user's space-time response vector with the noise subspace. The parameters are estimated by searching for the minimizers from the two-dimensional spectra as

$$\{\hat{\tau}_{1,1}, \hat{\theta}_{1,1}, ..., \hat{\tau}_{1,L}, \hat{\theta}_{1,L}\} = argmin_{\boldsymbol{\tau},\boldsymbol{\theta}} \ \hat{\mathbf{h}}_{1,l}^H \hat{\mathbf{U}}_n \hat{\mathbf{U}}_n^H \hat{\mathbf{h}}_{1,l} \ . \tag{69}$$

However, the estimated eigenvalues/eigenvectors got from the sample covariance matrix results in a biased parameter estimation. The quality of the estimated parameters is of the utmost importance. The cramer-rao lower bound (CRLB) is by far the most commonly used measure for accuracy. An estimator is said to be efficient if the estimator achieves the CRLB. [62] studies the performance of MUSIC for DOA estimation, and analyzes the statistical efficiency. To achieve the best asymptotic performance, the source signals in the space array model must be uncorrelated. The degradation of MUSIC performance for correlated signals in the space array model (1) have been studied in [22] [45] [62] [63] [85] [86]. In [48], the conditional CRLB is derived for unbiased two-dimensional code acquisition estimator.

3.3.2 ESPRIT

ESPRIT is another subspace method [40] [56]. It initially uses two identical arrays to perform the DOA estimation. ESPRIT requires the two arrays to form matched pairs, and utilizes the rotational invariance property of the underlying signal subspace. The signal subspace is obtained by the translational invariance of the antenna arrays. ESPRIT is a computationally efficient method which does

not need an exhaustive search through all directions to estimate the DOAs. It reduces the computational and storage requirement of MUSIC for DOA estimation. One drawback of ESPRIT is that the offset between the pairs must be known exactly. [35] gives a performance investigation. Other versions, referred to as total least squares TLS-ESPRIT and multi-invariance ESPRIT can be seen form [57] and [84].

As ESPRIT is considered for two-dimensional code acquisition, two methods, termed as shift-invariance joint angle and delay estimation (SI-JADE) and joint angle and delay estimation (JADE-ESPRIT), are exploited in [71] [72] [73] [74] in wireless communication systems. The first step of the two methods is to perform a pre-processing operation on the received signals. The pre-processing operation maps time delays into phase shifts in the frequency domain by discrete fourier transform (DFT). After the pre-processing operation, SI-JADE method smooths the resulting channel matrix to form a block Hankel matrix. Consequently, the problem for two-dimensional code acquisition is solved by using 2D ESPRIT. On the contrary, JADE-ESPRIT has no requirement for reshaping the received signals. Using SI-JADE and JADE-ESPRIT, the time delays and DOAs can be automatically paired under a single user multiple path transmission system.

4 TWO-DIMENSIONAL CODE ACQUISITION

In this chapter, independent component analysis (ICA) is firstly introduced and applied to the two-dimensional code acquisition in section one. Then, in section two an EV-t algorithm is addressed. After the description of the two algorithms, the seven publications attached to the thesis are summarized. Finally, in section four asymptotic statistical properties of MUSIC are analyzed in the special case that each user has two resolvable paths, and the analysis is based on the assumption that the space-time response vectors corresponding to distinct set $\{\theta, \tau\}$ are linearly independent.

4.1 ICA for two-dimensional code acquisition

Blind source separation (BSS) has been widely studied for separating individual signals from the observed mixture. In general, the separation of the individual signals depends only on the observed mixture with little prior knowledge about the statistics of the individual signals and/or the mixing process. As one approach of BSS, ICA is widely studied [3] [19] and its application could be originated form many different fields, such as digital images, document databases, economic indicators and psychometric measurements. Telecommunications is also a one ICA application area, in which the source signal is transmitted from a transmitter, through a medium, to a receiver. In this section, a basic introduction of ICA is given first. Then FastICA algorithm is presented and applied for two-dimensional code acquisition. After that, one modification of ICA is exploited and used for two-dimensional code acquisition.

4.1.1 Basic introduction of ICA

Data model of ICA

ICA [19] is a computational method to recover the observed signals into components (e.g. source signals) which are defined as statistically independent and nongaussian. A linear data model is generally used in ICA to transform the statistically independent source signals to a set of observed random variables. The linear ICA data model can be expressed as

$$\mathbf{x}_i = \mathbf{J}\mathbf{s}_i + \mathbf{n}_i \ . \tag{70}$$

Here $\mathbf{x}_i$ is the observed signal vector, which is generated by the mixing matrix $\mathbf{J}$ and the source signal vector $\mathbf{s}_i$. Each variable in the observed signal vector $\mathbf{x}_i$ is generated as a sum of the source variables of $\mathbf{s}_i$ weighted by one basic vector of mixing matrix $\mathbf{J}$, e.g. $x_{i,m} = j_{m,1}s_{i,1} + \cdots + j_{m,n}s_{i,n} + \cdots + j_{m,N}s_{i,N}$. In (70), the dimension of $\mathbf{x}_i$ is $M \times 1$, the dimension of $\mathbf{s}_i$ is $N \times 1$, and the dimension of the mixing matrix $\mathbf{J}$ is $M \times N$.

For clearly separating the source signals or identifying the mixing vector from the observed signals, some assumptions for the above linear ICA data model are made as following [19]:

s1. The source signals in source vector $\mathbf{s}_i$ are assumed statistically independent variables or in practice as independent as possible.

s2. At most one source signal is with gaussian distribution.

s3. The mixing matrix $\mathbf{J}$ is required to be a full rank matrix.

Two processing steps of ICA

The basic idea for the separation of the source signals is to transform the observed signal with the inverse of the mixing matrix. As $\mathbf{J}$ is assumed invertible, the recovery of the independent source signals can be performed as

$$\hat{\mathbf{s}}_i = \mathbf{T}\mathbf{x}_i \ , \tag{71}$$

where $\mathbf{T} = \mathbf{J}^{-1}$. However, the un-mixing matrix $\mathbf{T}$ can not be got directly from $\mathbf{J}$, because $\mathbf{J}$ is unknown. Typically, the recovery of the source signals by ICA is processed by two steps as showed in Figure 3.

First step: whitening data For good separation, whitening the observed signals is crucial [19]. It can be achieved by principal component analysis (PCA) or singular value decomposition (SVD). In general, whitening the observed signals makes ICA converge faster and be more stable. Meanwhile, the dimensionality reduction is achieved by crossing out the smallest eigenvalues, and the noise can be mitigated simultaneously. This leads to the simplification and reduction of the complexity for the actual iterative algorithm.

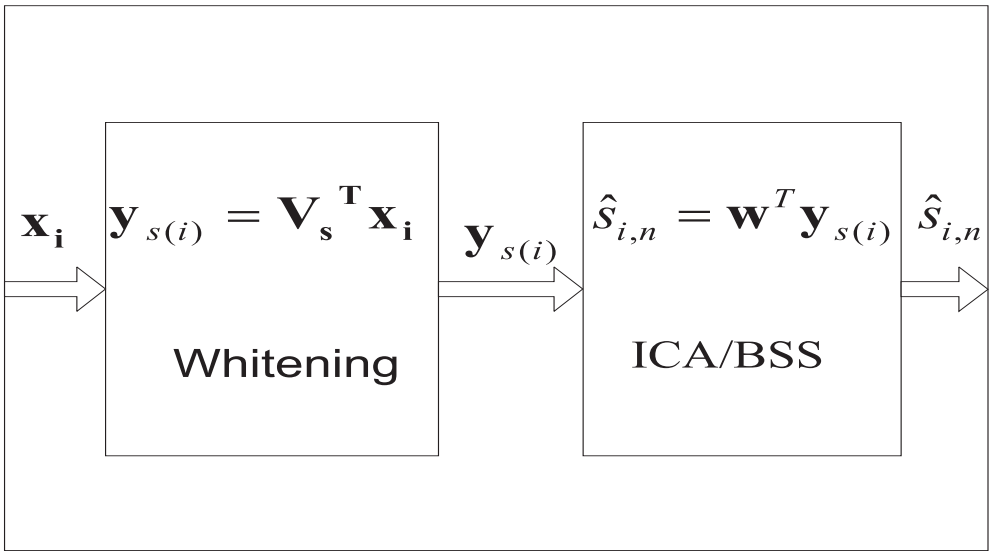

FIGURE 3 The illustration of processing steps of ICA.

Whiteness is slightly stronger than uncorrelatedness. In addition to the requirement of uncorrelatedness, the variances of the whitened data is further required to be unity. The whitening operation can be performed by second-order statistics, and forms an orthogonal matrix. The whitening operation is explained below.

First, whitening the observed signals according to

$$\mathbf{y}_i = \mathbf{V}\mathbf{x}_i \ , \tag{72}$$

where the vector $\mathbf{y}_i$ is the whitened data. $\mathbf{V}$ is the whitening matrix, which should be chosen such that $E\{\mathbf{y}_i\mathbf{y}_i^T\} = \mathbf{I}$. At first, covariance matrix of $\mathbf{x}_i$ is considered and expressed as

$$E\{\mathbf{x}_i\mathbf{x}_i^T\} = \mathbf{U}\mathbf{\Lambda}\mathbf{U}^T \ , \tag{73}$$

where the matrices $\mathbf{U}$ and $\mathbf{\Lambda}$ contain eigenvectors and eigenvalues, respectively. Due to the orthogonality of the eigenvectors i.e. $\mathbf{u}_q^T\mathbf{u}_p = 0$ for $q \neq p$, if the whitening matrix $\mathbf{V}$ is chosen as

$$\mathbf{V} = \mathbf{\Lambda}^{-\frac{1}{2}}\mathbf{U}^T \ , \tag{74}$$

we get

$$E\{\mathbf{y}_i\mathbf{y}_i^T\} = \mathbf{V}E\{\mathbf{x}_i\mathbf{x}_i^T\}\mathbf{V}^T = \mathbf{\Lambda}^{-\frac{1}{2}}\mathbf{U}^T\mathbf{U}\mathbf{\Lambda}\mathbf{U}^T\mathbf{U}\mathbf{\Lambda}^{-\frac{1}{2}} = \mathbf{I} \ . \tag{75}$$

As the whitening matrix is performed in the signal subspace, the whitening matrix is rewritten as $\mathbf{V}_s = \mathbf{\Lambda}_s^{-\frac{1}{2}}\mathbf{U}_s^T$, and the whitened data can be represented as

$$\mathbf{y}_{s(i)} = \mathbf{V}_s\mathbf{x}_i = \mathbf{\Lambda}_s^{-\frac{1}{2}}\mathbf{U}_s^T\mathbf{x}_i \ . \tag{76}$$

Second step: blind source separation After the whitening operation, the components of $\mathbf{y}_{s(i)}$ are uncorrelated. For seeking mutually independent components, several approaches, e.g. maximization of nongaussianity, maximum likelihood estimation, minimization of mutual information, tensorial methods, and nonlinear decorrelation and nonlinear PCA etc., are introduced in [19]. Below, FastICA algorithm based on nongaussianity is introduced.

Non-gaussianity: To recover one source signal, we look for a linear combination $\mathbf{w}^T\mathbf{y}_{s(i)}$ to maximize nongaussianity as

$$\hat{s}_{i,n} = \mathbf{w}^T\mathbf{y}_{s(i)} = \mathbf{w}^T\mathbf{V}_s\mathbf{x}_i = \mathbf{w}^T\mathbf{V}_s\mathbf{J}\mathbf{s}_i \triangleq \mathbf{q}^T\mathbf{s}_i \ . \tag{77}$$

From (77), we can see that $\hat{s}_{i,n}$ is a linear combination of the source signals in the source vector $\mathbf{s}_i$. Hence $\mathbf{q}^T\mathbf{s}_i$ is more gaussian than any of the source signals of $\mathbf{s}_i$, and become least gaussian when it in fact equals one of the source signals of $\mathbf{s}_i$. However, if only one component of $\mathbf{q}$ is nonzero, one source signal in the source vector $\mathbf{s}_i$ can be estimated. Therefore, $\mathbf{w}$ is defined to maximize the nongaussianity of $\mathbf{w}^T\mathbf{y}_{i(s)}$. Each output, e.g. $\hat{s}_{i,n}$, can be regarded as an approximation of one of the source signals. In this situation, one source signal is recovered.

FastICA: Fourth-order statistics kurtosis is used in FastICA algorithm [18], and its expression is

$$kurt(v) = E\{v^4\} - 3(E\{v^2\})^2 \ , \tag{78}$$

where v is defined as a zero-mean random variable. For a gaussian random variable, kurtosis is zero. The fourth moment of gaussian random variable v equals to $3(E\{v^2\})^2$. For most nongaussian random variable, kurtosis is nonzero.

We define a linear combination $\mathbf{w}^T\mathbf{y}_{s(i)}$ to seek for a non-gaussianity maximizer for the whitened data $\mathbf{y}_{s(i)}$. Since $\mathbf{w}^T\mathbf{y}_{s(i)} = \mathbf{w}^T\mathbf{V}_s\mathbf{J}\mathbf{s}_i = \mathbf{q}^T\mathbf{s}_i$, we have $\mathbf{q} = (\mathbf{V}_s\mathbf{J})^T\mathbf{w}$, and therefore

$$||\mathbf{q}||^2 = (\mathbf{w}^T\mathbf{V}_s\mathbf{J})(\mathbf{J}^T\mathbf{V}_s^T\mathbf{w}) = ||\mathbf{w}||^2 \ . \tag{79}$$

We see that constraining $\mathbf{q}$ to lie on the unit sphere is equivalent to constraining $\mathbf{w}$ to be on the unit sphere as well. Under the simpler constrain of $||\mathbf{w}|| = ||\mathbf{q}|| = 1$, we replace v with $\mathbf{w}^T\mathbf{y}_{i(s)}$ in (78). Thus, we have

$$kurt(\mathbf{w}^T\mathbf{y}_{s(i)}) = E\{(\mathbf{w}^T\mathbf{y}_{s(i)})^4\} - 3E\{(\mathbf{w}^T\mathbf{y}_{s(i)})^2\}^2 = E\{(\mathbf{w}^T\mathbf{y}_{s(i)})^4\} - 3 \parallel \mathbf{w} \parallel^4 \ . \tag{80}$$

For maximizing the absolute value of $kurt(\mathbf{w}^T\mathbf{y}_{i(s)})$, gradient method can be used as following

$$\frac{\partial |kurt(\mathbf{w}^T\mathbf{y}_{s(i)})|}{\partial \mathbf{w}} = 4sign(kurt(\mathbf{w}^T\mathbf{y}_{s(i)}))[E\{\mathbf{y}_{s(i)}(\mathbf{w}^T\mathbf{y}_{s(i)})^3\} - 3\mathbf{w} \parallel \mathbf{w} \parallel^2] \ . \tag{81}$$

Equal to the gradient of kurtosis of (81), a more efficient fixed point iteration is derived as

$$\mathbf{w} \propto E\{\mathbf{y}_{s(i)}(\mathbf{w}^T\mathbf{y}_{s(i)})^3\} - 3\mathbf{w} \parallel \mathbf{w} \parallel^2 \ , \tag{82}$$

where $\propto$ stands for "is proportional to". The convergence is carried out by adding gradient to the direction of $\mathbf{w}$.

The fixed-point algorithm for ICA can be concluded in the following steps [19]

1. Take a random initial vector $\mathbf{w}(0)$ of norm 1. Let t=1.

2. Let $\mathbf{w}(t) = E\{\mathbf{y}_{s(i)}(\mathbf{w}(t-1)^T\mathbf{y}_{s(i)})^3\} - \gamma\mathbf{w}(t-1)$.

3. Divide $\mathbf{w}(t)$ by its norm.

4. If $\mathbf{w}(t)^T\mathbf{w}(t-1)$ is not close enough to 1, let t=t+1 and go back to step 2, otherwise, output the vector $\mathbf{w}(t)$.

The above FastICA algorithm is designed for real-valued data, and $\gamma = 3$. Actually in [4], [7], and [30], FastICA algorithm is considered for complex-valued data. Compared to the case of real-valued mixture, $\gamma = 2$ is for complex-valued mixture.

4.1.2 FastICA algorithm for two-dimensional code acquisition

Comparing the linear ICA data model (70) and the DS-CDMA array model (35), we see the source signals $\mathbf{s}_i$ of (70) corresponds to the transmitted symbols $\mathbf{b}_i$ of (35). They have the same assumption descriptions which are *As1* on page 31 and *s1* on page 42. The linear mixing matrix $\mathbf{J}$ of (70) corresponds to $\mathbf{H}$ in (35) which contain channel parameters e.g. time delays and DOAs. Furthermore, the observed signal vector $\mathbf{x}_i$ of (70) corresponds to $\mathbf{r}_i$ of (35). Due to the similarity of the two data models, ICA can be applied into DS-CDMA systems.

The goal of a blind separation method is to recover/separate the source signals from the observed mixture (e.g. received signals). As ICA is applied into DS-CDMA systems, it is initially considered for separating the desired signal from the interfering signals. In literature, e.g. [9], [11], [51], [52], [53], [54], and [55], ICA is applied to the blind multiuser detection problem.

Due to the source signals are influenced by the realities of the surrounding environment, the observed mixture contains also number of unknown parameters. Instead of separating the source signals from the observed mixture , we span the application of ICA for parameter estimation. For obtaining an unambiguous solution, a full column rank assumption on the matrix $\mathbf{J}$ is required. In other words, the question of parameter identifiability is thus reduced to investigating under what conditions the array covariance uniquely determines the signal parameters. The general assumption *s3* made in the linear ICA data model just satisfies the requirement.

As ICA is applied to the two-dimensional code acquisition, the first step is to perform the whitening operation using a second-order tool. The whitened data can be computed as

$$\mathbf{y}_{s(i)} = \hat{\mathbf{\Lambda}}_s^{-1/2}\hat{\mathbf{U}}_s^H\mathbf{r}_i \ . \tag{83}$$

Due to the uncorrelatedness of the symbols, i.e. $E\{\mathbf{b}_i\mathbf{b}_i^T\} = \mathbf{I}$, we look for $\mathbf{I} = E\{\mathbf{y}_{s(i)}\mathbf{y}_{s(i)}^H\} = E\{\mathbf{W}\mathbf{b}_i\mathbf{b}_i^T\mathbf{W}^H\} = \mathbf{W}\mathbf{W}^H$. Utilizing FastICA algorithm, the goal hence is to extract the desired ICA basis vector from the mixing matrix. However,

extracting the vectors of $\mathbf{W}$ in a specified order is not possible. The reason is that the statistical features of the source signals are similar to each other, they are defined as mutually independent and nongaussian. Meanwhile, the statistical feature of each channel coefficient in wireless transmission could not be defined. Hence, the available training sequence in wireless communication systems can be used as prior information to perform the identification for one specific vector of $\mathbf{W}$. The ICA iteration for one user, say the first user, can be initialized by using known symbols as

$$\mathbf{w}(0) = E\{\mathbf{y}_{s(i)} b_{1,i}\} = E\{\mathbf{W}\mathbf{b}_i b_{1,i}\} = \mathbf{W}[0100...0]^T \ . \tag{84}$$

For updating $\mathbf{w}(0)$, FastICA algorithm is used and performed until $|\mathbf{w}(t)^H \mathbf{w}(t-1)|$ is close enough to 1. The operation is as

$$\mathbf{w}(t) \ = \ E\{\mathbf{y}_{s(i)} (\mathbf{w}(t-1)^H \mathbf{y}_{s(i)}) * |\mathbf{w}(t-1)^H \mathbf{y}_{s(i)}|^2\} - \gamma \mathbf{w}(t-1) \ , \tag{85}$$

here γ is defined as 2 , and $|\cdot|$ stands for absolute value here. Due to $\mathbf{w}^H(0)\mathbf{y}_{s(i)} = \hat{b}_{1,i}$, this step actually equals to find maximum nongaussianity for independent components.

After that, the two-dimensional code acquisition can then be performed by searching the maximum output power from the two-dimensional spectrum as

$$\{\hat{\tau}_1, \hat{\theta}_1\} = argmax_{\tau,\theta} \ \mathbf{w}^H(t) \hat{\mathbf{U}}_s^H \hat{\mathbf{\Lambda}}_s^{-1/2} \hat{\mathbf{h}}_1 \ . \tag{86}$$

In the work of the thesis, FastICA algorithm is considered and applied for two-dimensional code acquisition in the special case of the DS-CDMA array model (35) with single path (L=1) and $a_{k,l,i} = a_{k,i} = a_k$ is constant during a block of symbols, hence the first user's space-time code vector is defined as $\hat{\mathbf{h}}_1 = \mathbf{c}_{1,1} \otimes \mathbf{a}_{1,1} = \mathbf{c}_1 \otimes \mathbf{a}_1$.

The utilization of FastICA algorithm in wireless communications is bounded within a static non-fading environment. The reason is that a necessary and sufficient condition, which is at most one gaussian signal among the source signals, is required in ICA. In wireless DS-CDMA communication systems, fading channel is often inevitable and causes the transmitted signals to obey more and more gaussian distribution. Hence, ICA is hardened to the fading channel. Below, ICA-FS as an effective method is suggested to solve the problem in that case.

4.1.3 ICA-FS for CDMA

With single path assumption, the received signals (35) can be decomposed into four parts called first user's signal, ISI, MAI, and noise interference as

$$\begin{aligned}\mathbf{r}_i &= \underbrace{\mathbf{h}_1 a_{1,i} b_{1,i}}_{desiredterm} + \underbrace{\underline{\mathbf{h}}_1 a_{1,i-1} b_{1,i-1} + \overline{\mathbf{h}}_1 a_{1,i+1} b_{1,i+1}}_{ISI} \\ &+ \underbrace{\sum_{k=2}^{K} (\underline{\mathbf{h}}_k a_{k,i-1} b_{k,i-1} + \mathbf{h}_k a_{k,i} b_{k,i} + \overline{\mathbf{h}}_k a_{k,i+1} b_{1,i+1})}_{MAI} \\ &+ \underbrace{\mathbf{n}_i}_{noiseterm} \quad .\end{aligned} \tag{87}$$

It can be further expressed as

$$\mathbf{r}_i = \mathbf{h}_1 a_{1,i} b_{1,i} + \mathbb{I}_{ISI(i)} + \mathbb{I}_{MAI(i)} + \mathbb{I}_{n(i)} \ . \tag{88}$$

The key point of the ICA-FS algorithm is to isolate the first user from the interferences. Hence, a pre-processing operation can at first be performed by multiplying $\mathbb{Z}$ on $\mathbf{r}_i$, and $\mathbb{Z}$ is given as [17]

$$\mathbb{Z} = \mathbf{I}_M \otimes diag(\mathcal{F}\mathbf{g}_1(0))^{-1}\mathcal{F} \ , \tag{89}$$

where $\mathbf{g}_1(0)$ is the code vector of the first user with time delay $\tau = 0$. $\mathcal{F}$ is $2N \times 2N$ dimensional fourier transform matrix, and has the form as

$$\mathcal{F} = [\underline{\boldsymbol{\psi}}^0, \underline{\boldsymbol{\psi}}^1, ..., \underline{\boldsymbol{\psi}}^{2N-1}] \quad , \tag{90}$$

where $\underline{\boldsymbol{\psi}} = [\psi^0, \psi^1, ..., \psi^{2N-1}]^T$ and $\psi = e^{-j(2\pi/2N)}$. Applying $\mathbb{Z}$ on $\underline{\mathbf{h}}_k$, $\mathbf{h}_k$, and $\overline{\mathbf{h}}_k$ leads to the time delays to be mapped to phase shifts in the frequency domain. For example, for a particular $\mathbf{h}_k$, we have

$$\mathbf{I}_M \otimes diag(\mathcal{F}\mathbf{g}_1(0))^{-1}\mathcal{F}\mathbf{h}_k = \mathbf{a}_k \otimes (diag(\mathcal{F}\mathbf{g}_1(0))^{-1} diag\mathcal{F}\mathbf{g}_k(0)\underline{\boldsymbol{\psi}}^{\tau_k}) \ . \tag{91}$$

If and only if $k = 1$, (91) can be simplified to $\mathbf{a}_1 \otimes \underline{\boldsymbol{\psi}}^{\tau_1}$.

Hence, by applying the same operation to the received data $\mathbf{r}_i$, the discretised signal vector is thus transformed to

$$\begin{aligned}\mathbf{r}_{FS(i)} &= \mathbb{Z}\mathbf{r}_i \\ &= \mathbb{Z}\mathbf{h}_1 a_{1,i} b_{1,i} + \mathbb{Z}\mathbb{I}_{ISI(i)} + \mathbb{Z}\mathbb{I}_{MAI(i)} + \mathbb{Z}\mathbb{I}_{n(i)} \\ &= \mathbf{a}_1 \otimes \underline{\boldsymbol{\psi}}^{\tau_1} a_{1,i} b_{1,i} + \mathbb{Z}\mathbb{I}_{ISI(i)} + \mathbb{Z}\mathbb{I}_{MAI(i)} + \mathbb{Z}\mathbb{I}_{n(i)} \ .\end{aligned} \tag{92}$$

Due to the low cross-correlations, the column of $\mathbf{H}_{FS}$ for $k \neq 1$, are with a lower norm. So the contribution of interferences is decreased.

After the pre-processing operation, the space-time array model (35) can be rewritten as

$$\mathbf{r}_{FS(i)} = \mathbf{H}_{FS}\mathbf{A}_i\mathbf{b}_i + \mathbf{n}_{FS(i)} \ . \tag{93}$$

The above function still obeys the DS-CDMA array model (35), and the linear ICA data model (70). We make a mark "FS" in the above function. $\mathbf{r}_{FS(i)}$ is the observed signals after the pre-processing operation, and $\mathbf{n}_{FS(i)}$ denotes the noise vector after the pre-processing operation. From (93), we see the pre-processing operation is actually performed on the matrix $\mathbf{H}$ of (35).

4.2 EV-t algorithm for two-dimensional code acquisition

In this section, the subspace-based algorithm EV-t is addressed for two-dimensional code acquisition.

For subspace-based methods, a general cost function can be defined for parameter estimation as

$$\{\hat{\tau}_{1,1}, \hat{\theta}_{1,1}, \cdots, \hat{\tau}_{1,L}, \hat{\theta}_{1,L}\} = argmax/argmin_{\boldsymbol{\tau},\boldsymbol{\theta}}\, \hat{\mathbf{h}}_{1,l}^H \mathcal{H}(\mathbf{R}) \hat{\mathbf{h}}_{1,l} \ . \tag{94}$$

Natural extensions of the general cost function can be achieved with different definitions of $\mathcal{H}(\mathbf{R})$, e.g. $\mathcal{H}(\mathbf{R}) = \hat{\mathbf{U}}_n \hat{\mathbf{U}}_n^H$ results in MUSIC algorithm, and $\mathcal{H}(\mathbf{R}) = \hat{\mathbf{U}}_n \hat{\mathbf{\Lambda}}_n^{-1} \hat{\mathbf{U}}_n^H$ results in EV algorithm. They look for the desired user's space-time response vector at the correct time delay and angle offset must be orthogonal to the noise subspace. Meanwhile, they are developed without any consideration to access the source signals.

However, the proposed EV-t algorithm has two different characters with the general subspace-based methods, e.g. MUSIC and EV. First of all, instead of searching the minimum projection of the desired signal's space-time response vector on the noise subspace, we search the maximum projection of the desired signal's space-time response vector on the signal subspace. Secondly, we utilize the training sequence. In digital communication systems, the modulation format of the transmitted signals is known to the receiver, although the transmitted symbol stream is unknown. In mobile communication systems, a known preamble may be added to the message for training purposes. Distinguish to the general subspace-based methods without considering any knowledge of the source signal, the proposed EV-t algorithm utilizes the support of the training sequence.

Hence, the weight vector of EV-t for two-dimensional code acquisition is defined as

$$\mathbf{w}_{EV-t} = \hat{\mathbf{U}}_s \hat{\mathbf{\Lambda}}_s^{-1} \hat{\mathbf{U}}_s^H \check{\mathbf{h}}_1 \ . \tag{95}$$

As we define $\hat{Z}(\theta, \tau) = \mathbf{w}_{EV-t}^H \hat{\mathbf{h}}_{1,l}$, the two-dimensional code acquisition can be performed as

$$\begin{aligned} \{\hat{\tau}_{1,1}, \hat{\theta}_{1,1}, ..., \hat{\tau}_{1,L}, \hat{\theta}_{1,L}\} &= argmax_{\boldsymbol{\tau},\boldsymbol{\theta}}\, \hat{Z}(\theta, \tau) \\ &= argmax_{\boldsymbol{\tau},\boldsymbol{\theta}}\, \mathbf{w}_{EV-t}^H \hat{\mathbf{h}}_{1,l} \ , \end{aligned} \tag{96}$$

In (95), $\check{\mathbf{h}}_1$ is the estimated space-time response vector by the help of training sequence. Due to the assumption *As1*, $E\{\mathbf{H}\mathbf{A}_i \mathbf{b}_i b_{1,i}\} = \sum_{l=1}^{L} \mathbf{h}_{1,l} a_{1,l,i}$. Hence the first user's training sequence $\mathbf{B}_1 = [b_{1,1}, ..., b_{1,I}]^T$ can be used to roughly estimate $\mathbf{h}_{1,l}$. Since then we have $\check{\mathbf{h}}_1 = \sum_{l=1}^{L} \mathbf{h}_{1,l} a_{1,l} + \check{\mathbf{n}}$, where $a_{1,l} = \sum_{i=1}^{I} a_{1,l,i}$.

The EV-t algorithm for two-dimensional code acquisition can be briefly described in three steps as following:

1. Eigen-decompose the sample correlation matrix $\hat{\mathbf{R}}_r = \frac{1}{I} \sum_{i=1}^{I} \mathbf{r}_i \mathbf{r}_i^H$ to form the mutual orthogonal signal subspace and noise subspace as

$$\hat{\mathbf{R}}_r = \hat{\mathbf{U}}_s \hat{\mathbf{\Lambda}}_s \hat{\mathbf{U}}_s^H + \hat{\mathbf{U}}_n \hat{\mathbf{\Lambda}}_n \hat{\mathbf{U}}_n^H \ . \tag{97}$$

2. Calculate $\mathbf{w}_{EV-t}$ by utilizing the training sequence of the first user. Due to uncorrelatedness of symbols, the weight vector of EV-t can be expressed as

$$\mathbf{w}_{EV-t} = \hat{\mathbf{U}}_s \hat{\mathbf{\Lambda}}_s^{-1} \hat{\mathbf{U}}_s^H \mathbf{R}\mathbf{B}_1 = \hat{\mathbf{U}}_s \hat{\mathbf{\Lambda}}_s^{-1} \hat{\mathbf{U}}_s^H \check{\mathbf{h}}_1 \ . \tag{98}$$

3. Perform the two-dimensional code acquisition by searching the maximum projections of the desired user's space-time response vector on the signal subspace. The parameters are estimated by searching the maximum peaks through a two-dimensional spectra as

$$\begin{aligned} \{\hat{\tau}_{1,1}, \hat{\theta}_{1,1}, ..., \hat{\tau}_{1,L}, \hat{\theta}_{1,L}\} &= argmax_{\boldsymbol{\tau},\boldsymbol{\theta}} \, \hat{Z}(\theta, \tau) \\ &= argmax_{\boldsymbol{\tau},\boldsymbol{\theta}} \, \mathbf{w}_{EV-t}^H \hat{\mathbf{h}}_{1,l} \ . \end{aligned} \tag{99}$$

If eigenvalues/eigenvectors are accurately estimated, L maximum peaks indicating space-time directions of the first user can be caught.

4.3 Overview of articles

This section summarizes the seven publications attached to the thesis. The publications are published as individual pieces of research in one journal paper and six conference papers. Three papers utilizing ICA based algorithms for two-dimensional code acquisition are included in the first subsection. The other four papers addressing the EV-t algorithm for two-dimensional code acquisition are contained in the second subsection.

4.3.1 ICA for channel parameter acquisition

Traditionally, ICA searches a linear transformation on the observed variables, and results in a set of independent components. In this application only the source signals are of interest. However, instead of separating the source signals, we are more interested in using ICA for parameter estimation. Actually, in [10] [12], FastICA algorithm has been used for time delay estimation. In this thesis, the application of ICA for parameter estimation is extended. Publication I focuses on the application of ICA for two-dimensional code acquisition in DS-CDMA systems. Publication II presents a further exploited ICA to perform the two-dimensional code acquisition. Publication III demonstrates that the further exploited ICA is an efficient method for two-dimensional code acquisition when the wireless channel suffers from fading.

I. R. Wu, T. Ristaniemi, "Joint Time Delay and DOA Estimation in CDMA Communication Using FastICA Algorithm", In *Proceedings of the 8th International Conference on Cellular and Intelligent Communications(CIC 2003)*, Oct. 28-31, 2003, Seoul, Korea.

Generally, the spatial parameter DOA and the temporal parameter time delay are separately estimated. In wireless communication systems, each propagated signal is a function of time delay and DOA. Hence, this paper pays attention on the two-dimensional code acquisition.

Firstly, the data model in this paper is established as a special case of (35), while the path number of each user is set as $L = 1$ and the attenuation factors $a_{k,l,i} = a_{k,i} = a_k$ are constant during a block of symbols. In this case, the space-time array manifold $\mathbf{H} = [\underline{\mathbf{h}}_1, \mathbf{h}_1, \overline{\mathbf{h}}_1, ..., \underline{\mathbf{h}}_K, \mathbf{h}_K, \overline{\mathbf{h}}_K]$. The matrix $\mathbf{A}_i = \mathbf{A} = diag\{a_{1,i-1}, a_{1,i}, a_{1,i+1}, ..., a_{K,i-1}, a_{K,i}, a_{K,i+1}\}$ and the vector $\mathbf{b}_i = [b_{1,i-1}, b_{1,i}, b_{1,i+1}, \ldots, b_{K,i-1}, b_{K,i}, b_{K,i+1}]^T$. Due to the similarity of the linear ICA data model and the DS-CDMA array model, ICA is suggested and applied for two-dimensional code acquisition.

The conducted simulations are to investigate the performance of ICA on the effect of the increasing user numbers, SNR, and MAI. The simulation results show that, even if the channel contains more users, ICA can perform a clear parameter estimation especially for time delay with a much wider MAI region. In addition, the simulation results indicate that the performance of ICA can be enhanced especially with moderate/high SNR values.

II. T. Ristaniemi, R. Wu, "Interference Suppression for Spatial-Temporal Propagation Parameters Identification in Wireless Communications", In *Proceedings of the IEEE Communications, Circuits and Systems Conference (ICCCAS'04)*, pp. 1022-1026, June 27-29, 2004, Chengdu, China.

This paper exploits the ICA-FS algorithm for two-dimensional code acquisition. Similarly to the publication I, the data model established in this paper is a single path DS-CDMA array model (35), and the attenuation factors $a_{k,l,i} = a_k$ are constant during a block of symbols. The first step of the ICA-FS algorithm is to perform a pre-processing operation on the received signals $\mathbf{r}_i$. After the pre-processing operation, the space-time array model (35) is rewritten as

$$\mathbf{r}_{FS(i)} = \mathbf{H}_{FS}(\theta, \psi)\mathbf{A}\mathbf{b}_i + \mathbf{n}_{FS(i)} \ . \tag{100}$$

Then, ICA is utilized to perform the two-dimensional code acquisition on the above data model.

Using ICA, the whitening operation is processed as

$$\mathbf{y}_{FS(i)} = \hat{\mathbf{\Lambda}}_s^{-1/2}\hat{\mathbf{U}}_s^H\mathbf{r}_{FS(i)} \ . \tag{101}$$

Then, FastICA algorithm is used to update one specific basic vectors of the matrix $\mathbf{W}_{FS}$. The operation is processed as

$$\begin{aligned} \mathbf{w}_{FS(i)}(t) &= E\{\mathbf{y}_{FS(i)}(\mathbf{w}_{FS(i)}(t-1)^H\mathbf{y}_{FS(i)}) * |\mathbf{w}_{FS(i)}(t-1)^H\mathbf{y}_{FS(i)}|^2\} \\ &- \gamma\mathbf{w}_{FS(i)}(t-1) \ . \end{aligned} \tag{102}$$

Corresponding to the first user, the initial value is defined as $\mathbf{w}_{FS(i)}(0) = \mathbf{y}_{FS(i)}b_{1,i}$.

Finally, the two-dimensional code acquisition is processed as

$$\{\hat{\tau}_1, \hat{\theta}_1\} = argmax_{\tau,\theta} \mathbf{w}_{FS(i)}^H(t) \hat{\mathbf{\Lambda}}_{FS}^{-1/2} \hat{\mathbf{U}}_{FS}^H (\mathbf{a}_1 \otimes \underline{\boldsymbol{\psi}}^{\tau_1}) \ . \tag{103}$$

In this paper, we conduct the simulations to achieve an insight into the ICA-FS algorithm and examine its performance on the effect of the varying MAI, SNR, the frame length, and the number of users. Through the pre-processing operation, the interferences are effectively suppressed in the frequency domain. Hence, numerical results show that the ICA-FS algorithm usually reaches a better achieved probability acquisition than the traditional FastICA algorithm, especially for time delay estimation.

III. R. Wu, T. Ristaniemi, "Spatial-Temporal Propagation Parameter Estimation in the Asynchronous DS-CDMA Systems over Fading Channel", In *Proceedings of the IEEE Communications and Information Technologies Symposium (ISCIT 2004)*, pp. 166-170, Oct. 26-29, 2004, Sapporo, Japan.

In this paper, the data model is established with a single path assumption. As a mobile is moving, the wireless channel is no longer constant in time. With a high carrier frequency, the fading channel changes rapidly over time. Hence, the attenuation factors are defined approximately constant over the time span of only one symbol, and the matrix $\mathbf{A}_i = diag\{a_{1,i-1}, a_{1,i}, a_{1,i+1}, ..., a_{K,i-1}, a_{K,i}, a_{K,i+1}\}$. Due to the pre-processing operation, (35) has a new form as

$$\mathbf{r}_{FS(i)} = \mathbf{H}_{FS}(\theta, \psi)\mathbf{A}_i\mathbf{b}_i + \mathbf{n}_{FS(i)} \ . \tag{104}$$

Then, the whitening operation is processed on the above data model. After that, one specific basis vector of the matrix $\mathbf{W}$ corresponding to the first user is updated by FastICA algorithm, and the two-dimensional code acquisition is finally performed.

In this paper, the performed simulations for two-dimensional code acquisition are examined in an asynchronous direct sequence spread spectrum communication system with the presence of Rayleigh fading effects. The ICA-FS algorithm is tested in the cases of the varying number of antenna elements, MAI, SNR, and block length. Due to the pre-processing operation, the numerical simulations show ICA-FS may clearly generate better results, even through the computational complexity is almost the same as the traditional FastICA algorithm.

4.3.2 EV-t for channel parameter acquisition

As mentioned in section 4.2, EV-t is a subspace based method which utilizes the training sequence support. In publication VI, we apply EV-t for two-dimensional code acquisition in an uncorrelated multipath scenario. In publication V, the application of EV-t for two-dimensional code acquisition is not limited in uncorrelated multipath propagation, and its performance is analyzed in both an uncorrelated and coherent multipath environment. In publication VI, we derive a general

asymptotic statistical analysis of EV-t, e.g. the mean and variance of EV-t for two-dimensional code acquisition. Furthermore, in publication VII, a comparison of EV-t and MUSIC for two-dimensional code acquisition is given.

IV. R. Wu, T. Ristaniemi, "EV-t Method for Parameter Estimation in DS-CDMA Communications", In *Proceedings of the Third IEEE International Workshop on Intelligent Signal Processing (WISP'2005)*, pp. 328-333, Sep. 1-3, 2005, Faro, Portugal.

In wireless communication systems, the transmitted signal is propagated through a multipath to a receiver, hence in this paper the data model is established with the assumption that each user has L paths propagation. The attenuation factors are assumed to be approximate constant over the time span of only one symbol. In this paper, the correlation coefficient between the various paths from the same user is defined as e.g. $\rho_{k(l,l')} = E\{a_{k,l,i}a^*_{k,l',i}\}/E\{||a_{k,l,i}||\}E\{||a^*_{k,l',i}||\} = 0$. In this case the correlation matrix $\mathbf{R}_{f(i)} = \mathbf{f}_i\mathbf{f}_i^H = \mathbf{A}_i\mathbf{A}_i^H = \mathbf{R}_{A(i)}$ is diagonal.

In this paper, the EV-t algorithm is first presented. Utilizing the available training sequence, the two-dimensional code acquisition is performed as

$$\begin{aligned}\{\hat{\tau}_{1,1}, \hat{\theta}_{1,1}, ..., \hat{\tau}_{1,L}, \hat{\theta}_{1,L}\} &= argmax_{\boldsymbol{\tau},\boldsymbol{\theta}}\, \hat{Z}(\theta,\tau) \\ &= argmax_{\boldsymbol{\tau},\boldsymbol{\theta}}\, \mathbf{w}_{EV-t}^H \hat{\mathbf{h}}_{1,l}\ .\end{aligned} \tag{105}$$

The searched L maximum peaks through the two-dimensional spectrum indicate the sets of space-time parameters corresponding to the first user.

Then this paper analyzes the performance of the EV-t algorithm under the assumption of the uncorrelated multipath propagation environment. The limitations of the algorithm resulted from the perturbation on the estimated eigenvalue and eigenvectors in the signal subspace [44] [83], and the estimated $\check{\mathbf{h}}_1$ are addressed.

In this paper, EV-t is tested in the environment of an asynchronous DS-CDMA uplink channel where the received multi-user signals undergo a frequency selective Rayleigh fading. The simulations in this paper examine the performance of EV-t with the increasing length of training sequence and varying MAI. Generally, subspace based methods, e.g. MUSIC, require a large symbol collection to achieve the asymptotic regime. However, the simulation results tell the fact that the performance of EV-t does not suffer from the need for a large set of symbol collection. As the collected symbols only reaches $3KL$, a high probability acquisition is possible by using EV-t. Meanwhile, EV-t can perform parameter estimation in a high MAI environment.

V. R. Wu, T. Ristaniemi, "Semi-Blind Two-Dimensional Code Acquisition in CDMA Communications", *International Journal of Signal Processing*, Vol. 3, No. 1, pp. 30-38, 2006.

In this paper, the data model is established as (35). The correlation coefficients between the various paths are not limited to the uncorrelated case as publication IV did. The performance of EV-t for two-dimensional code acquisition is analyzed both in an uncorrelated and coherent multipath environment in DS-CDMA arrays.

In this paper, we first assume the correlation coefficients between the various paths from the same user are zeros, the mean of EV-t for the first user first path is derived as

$$\begin{aligned} E\{\mathbf{w}_{EV-t}^H \hat{\mathbf{h}}_{1,1}\}_{un} &= \check{\mathbf{h}}_1^H \sum_{d=1}^{D} E\{\hat{\mathbf{u}}_d \hat{\lambda}_d^{-1} \hat{\mathbf{u}}_d^H\} \hat{\mathbf{h}}_{1,1} \\ &= a_{1,1} \mathbf{h}_{1,1}^H \mathbf{u}_1 \lambda_1^{-1} \mathbf{u}_1^H \hat{\mathbf{h}}_{1,1} + \chi_1 a_{1,1} \mathbf{h}_{1,1}^H \mathbf{u}_1 \mathbf{u}_1^H \hat{\mathbf{h}}_{1,1} + O(\frac{1}{I^2}) \ , \end{aligned} \tag{106}$$

where $D = 3KL$. The perturbation coefficient χ_1 is given as

$$\chi_1 = \frac{1}{I}(\sum_{d=2}^{D} \frac{1}{(\lambda_1 - \lambda_d)} - \frac{\sigma^2(2NM - D)}{(\lambda_1 - \sigma^2)^2}) \ . \tag{107}$$

As the correlation relationships between the various paths from the same user are coherent, the mean of EV-t for the first user first path is derived as

$$\begin{aligned} E\{\mathbf{w}_{EV-t}^H \hat{\mathbf{h}}_1\}_{co} &= \check{\mathbf{h}}_1^H \sum_{d=1}^{D} E\{\hat{\mathbf{u}}_d \hat{\lambda}_d^{-1} \hat{\mathbf{u}}_d^H\} \hat{\mathbf{h}}_{1,1} \\ &= a_{1,1} \mathbf{h}_{1,1}^H \mathbf{u}_1 \lambda_1^{-1} \mathbf{u}_1^H \hat{\mathbf{h}}_{1,1} + \chi_1 a_{1,1} \mathbf{h}_{1,1}^H \mathbf{u}_1 \mathbf{u}_1^H \hat{\mathbf{h}}_{1,1} \\ &+ \sum_{l=2}^{L} (a_{1,l} \lambda_1^{-1} + \chi_l a_{1,l}) \mathbf{h}_{1,l}^H \mathbf{u}_1 \mathbf{u}_1^H \hat{\mathbf{h}}_{1,1} + O(\frac{1}{I^2}) \ , \end{aligned} \tag{108}$$

where the perturbation coefficient χ_l is given as

$$\chi_l = \frac{1}{I}(\sum_{\substack{d=1 \\ d \neq l}}^{D} \frac{1}{(\lambda_l - \lambda_d)} - \frac{\sigma^2(2NM - D)}{(\lambda_l - \sigma^2)^2}) \ . \tag{109}$$

This paper indicates that the performance of EV-t depends highly on the coefficients $a_{1,l}$ and perturbation coefficients χ_l for $l = 1, ..., L$. Due to $a_{1,l}$ is integrity of $a_{1,l,i}$, its probability distribution can not be defined. Hence, the performance degradation can be caused by $a_{1,l}$ with increasing length of training sequence I.

VI. R. Wu, T. Ristaniemi, "The Performance Analysis of EV-t method for Two-Dimensional Code Acquisition", In *Proceedings of the First IEEE Workshop on Computational Advances in Multi-Sensor Adaptive Processing (CAMSAP'2005)*, pp. 229-232, Dec. 13-15, 2005, Puerto Vallarta, Jalisco State, Mexico.

In this paper the data model is established as (35), and the correlation coefficient between the various paths from the same user is defined as $0 \leq \rho_{k(l,l')} \leq 1$.

Due to the high-correlation/coherency of the various paths, the correlation matrix $\mathbf{R}_{f(i)} = \mathbf{f}_i\mathbf{f}_i^H = \mathbf{A}_i\mathbf{A}_i^H = \mathbf{R}_{A(i)}$ has a rank reduction.

First, this paper gives an overview of the EV-t algorithm. Then, this paper presents a rigorous statistical analysis for the EV-t algorithm. The performance analysis of the EV-t algorithm given in publications IV and V is limited to uncorrelated and coherent propagation environments. This paper relaxes this limitation, and a general asymptotic statistical analysis, e.g. the mean of the EV-t algorithm for the two-dimensional code acquisition is derived as

$$\begin{aligned} E\{\hat{Z}(\theta,\tau))\} &= E\{\mathbf{w}_{EV-t}^H\hat{\mathbf{h}}_{1,1}\} \qquad (110)\\ &= \sum_{d=1}^{D}\frac{1}{\lambda_d}\check{\mathbf{h}}_1^H\mathbf{u}_d\mathbf{u}_d^H\hat{\mathbf{h}}_{1,1} - \frac{1}{I}\sum_{d=1}^{D}\frac{\sigma^2(2NM-D)}{(\lambda_d-\sigma^2)^2}\check{\mathbf{h}}_1^H\mathbf{u}_d\mathbf{u}_d^H\hat{\mathbf{h}}_{1,1}\\ &+ \frac{1}{I}\sum_{d=1}^{D}\sum_{\substack{f=1\\ f\neq d}}^{D}\frac{1}{(\lambda_d-\lambda_f)}\check{\mathbf{h}}_1^H\mathbf{u}_d\mathbf{u}_d^H\hat{\mathbf{h}}_{1,1} + O(\frac{1}{I^2}) \ . \end{aligned}$$

The performance of the EV-t algorithm is tested in the environment of an asynchronous DS-CDMA system with a frequency selective Rayleigh fading channel. The conducted simulations in this paper examine the behavior of EV-t as a function of correlation coefficient varying from 0.1 to 1. Meanwhile, EV-t is examined in the effect of MAI in the coherent multipath propagation environment. The simulation results show EV-t suits the two-dimensional code acquisition well in a high-correlated/coherent multipath propagation environment without knowing the correlation relationship between the various paths from the same user, and it is a more powerful estimator to resist high MAI. We should mention here that the simulations are examined with a small received set of samples (symbols).

VII. R. Wu, T. Ristaniemi, "Performance Comparison of EV-t and MUSIC for Two-Dimensional Code Acquisition", In *Proceedings of IEEE International Symposium on Wireless Pervasive Computing 2006 (ISWPC'06)*, pp. 1-5, Jan. 16-18, 2006, Phuket, Thailand.

In this paper, the performance of the EV-t algorithm is compared to the traditional MUSIC algorithm, as they are used for the two-dimensional code acquisition. We use $\hat{Q}(\theta,\tau)$ to present MUSIC algorithm for two-dimensional code acquisition. Imitating [44], the mean of $\hat{Q}(\theta,\tau)$ can be given as

$$\begin{aligned} & E\{\hat{Q}(\theta,\tau)\} \qquad (111)\\ = \ & Q(\theta,\tau) + \frac{\sigma^2}{IX}\sum_{d=1}^{D}\frac{\lambda_d}{(\lambda_d-\sigma^2)^2}[(2NM-D)|\hat{\mathbf{h}}_{1,l}^H\mathbf{u}_d|^2 - Q(\theta,\tau)] + O(\frac{1}{I^2}) \ . \end{aligned}$$

If σ^2 is small enough, the performance of MUSIC does well with one order of λ_d. In this paper, the eigenvalues are further analyzed. It proves that the eigenvalues are proportional to the signal power, and the length of space-time response vector. The length of a space-time response vector is a product of the processing gain and the number of antenna elements.

The simulations in this paper examine the behavior of MUSIC and EV-t methods as a function of the number of users with different lengths of space-time response vectors. Although the performance of MUSIC has a great improvement with the increasing length of the space-time response vector, it still can not achieve high probability acquisition as EV-t in a high MAI environment.

4.4 Further analysis

In general, the array response vectors corresponding to different θ are assumed linearly independent. However it is a weak assumption to equivalently keep the array manifold to be a full column rank [62]. Hence, a reasonable consideration that low correlation coefficient, e.g. ρ_s, exists between two array response vectors. In this thesis, the array response vector is replaced by the space-time response vector in the DS-CDMA array model. Each space-time response vector, e.g. $\mathbf{h}_{k,l}$, is a combination of the array response vector $\mathbf{a}_{k,l}$ determined by the array geometry, and the code vector $\mathbf{c}_{k,l}$ depending on the pseudorandom code sequence. [48] assumes that the columns in space-time array manifold are linearly independent. In Appendix 1, we prove, compared to the correlation coefficients of array response vectors, the correlation coefficients of space-time response vectors have, e.g. $\frac{1}{\sqrt{N}}$, degradation in the DS-CDMA array model. Hence, we can say that the assumption of linear independence for the space-time response vectors is stronger with the increasing processing gain N. This section gives some detailed performance analysis of MUSIC for two-dimensional code acquisition, and the analysis is based on the assumption that the processing gain N is large enough. To simplify the complex calculation, the analysis on the asymptotic statistical properties of MUSIC is derived in the special case that each user has two resolvable paths.

Due to the eigenvalues λ_d and $|\mathbf{h}_{1,l}^H \mathbf{u}_d|^2$, $d = 1, ..., D$ and $l = 1, 2$, are principally important for asymptotic statistical analysis, in this section λ_d and $|\mathbf{h}_{1,l}^H \mathbf{u}_d|^2$ for $d = 1, ..., D$ and $l = 1, 2$, are primarily examined. Then the asymptotic statistical properties of MUSIC for two-dimensional code acquisition are derived later on.

4.4.1 Array structure decomposition

At first, we use $\dot{\lambda}_d = \lambda_d - \sigma^2$ to denote the noise free eigenvalue. In this case,

$$\mathbf{H}\mathbf{R}_{A(i)}\mathbf{H}^H \triangleq \mathbf{U}_s \dot{\mathbf{\Lambda}}_s \mathbf{U}_s^H = \sum_{d=1}^{D} \mathbf{u}_d \dot{\lambda}_d \mathbf{u}_d^H \quad . \tag{112}$$

Due to multiple users share the same channel in DS-CDMA systems, $\mathbf{H}\mathbf{R}_{A(i)}\mathbf{H}^H$ is a high order matrix. It is very complex to calculate $\dot{\lambda}_d$ and $|\mathbf{h}_{1,l}^H \mathbf{u}_d|^2$ for $d = 1, ..., D$ and $l = 1, 2$. Therefore, the evaluation process is divided into two steps. The first

step is to reshape the manifold matrix $\mathbf{H}$, the matrix $\mathbf{A}_i$, and the vector $\mathbf{b}_i$. Meanwhile, the received data $\mathbf{r}_i$ is unvaried. The second step is to evaluate $|\mathbf{h}_{1,l}^H \mathbf{u}_d|^2$ for $d = 1, ..., D$ and $l = 1, 2$, and the sum and product of the noise free eigenvalues. In the first step, the new formed correlation matrix of $\mathbf{H}\mathbf{A}_i\mathbf{b}_i$ is separated to several block matrices. This leads the evaluation of $\dot{\lambda}_d$ and $|\mathbf{h}_{1,l}^H \mathbf{u}_d|^2$, for $d = 1, ..., D$ and $l = 1, 2$, to be simplified. Such that as showed in the second step, whose $\dot{\lambda}_d$ and $|\mathbf{h}_{1,l}^H \mathbf{u}_d|^2$ only correspond to the first user are needed to be evaluated.

First step

To simplify the calculation, $\mathbf{H}\mathbf{A}_i\mathbf{b}_i$ is firstly rewritten as

$$\mathbf{H}\mathbf{A}_i\mathbf{b}_i \triangleq \tilde{\mathbf{H}}\tilde{\mathbf{A}}_i\tilde{\mathbf{b}}_i \ . \tag{113}$$

$\mathbf{H}$, $\mathbf{A}_i$, and $\mathbf{b}_i$ are re-expressed as $\tilde{\mathbf{H}}$, $\tilde{\mathbf{A}}_i$, and $\tilde{\mathbf{b}}_i$ respectively. $\tilde{\mathbf{H}} = [\underline{\mathbf{H}}_1, \mathbf{H}_1, \overline{\mathbf{H}}_1, \cdots, \underline{\mathbf{H}}_K, \mathbf{H}_K, \overline{\mathbf{H}}_K]$, where $\underline{\mathbf{H}}_k = [\underline{\mathbf{h}}_{k,1}, \underline{\mathbf{h}}_{k,2}]$, $\mathbf{H}_k = [\mathbf{h}_{k,1}, \mathbf{h}_{k,2}]$, and $\overline{\mathbf{H}}_k = [\overline{\mathbf{h}}_{k,1}, \overline{\mathbf{h}}_{k,2}]$. Correspondingly $\tilde{\mathbf{A}}_i = diag\{\underline{\mathbf{A}}_1, \mathbf{A}_1, \overline{\mathbf{A}}_1, ..., \underline{\mathbf{A}}_K, \mathbf{A}_K, \overline{\mathbf{A}}_K\}$, where $\underline{\mathbf{A}}_k = [a_{k,1,i-1}a_{k,2,i-1}]^T$, $\mathbf{A}_k = [a_{k,1,i}a_{k,2,i}]^T$, $\overline{\mathbf{A}}_k = [a_{k,1,i+1}a_{k,2,i+1}]^T$. $\tilde{\mathbf{b}}_i$ has same form as $\mathbf{b}_i$. By the assumptions *As1* and *As2*, the correlation matrix of $\tilde{\mathbf{H}}\tilde{\mathbf{A}}_i\tilde{\mathbf{b}}_i$ can be expressed as

$$\begin{aligned} &[\underline{\mathbf{H}}_1, \mathbf{H}_1, \overline{\mathbf{H}}_1, \cdots, \underline{\mathbf{H}}_K, \mathbf{H}_K, \overline{\mathbf{H}}_K] \\ &diag[\underline{\mathbf{R}}_{A1}, \mathbf{R}_{A1}, \overline{\mathbf{R}}_{A1}, ..., \underline{\mathbf{R}}_{AK}, \mathbf{R}_{AK}, \overline{\mathbf{R}}_{AK}] \\ &[\underline{\mathbf{H}}_1, \mathbf{H}_1, \overline{\mathbf{H}}_1, \cdots, \underline{\mathbf{H}}_K, \mathbf{H}_K, \overline{\mathbf{H}}_K]^H \ , \end{aligned} \tag{114}$$

where

$$\underline{\mathbf{R}}_{Ak} = \begin{pmatrix} a'_{k,(1,1),i-1} & a'_{k,(1,2),i-1} \\ a'_{k,(2,1),i-1} & a'_{k,(2,2),i-1} \end{pmatrix}, \tag{115}$$

$$\mathbf{R}_{Ak} = \begin{pmatrix} a'_{k,(1,1),i} & a'_{k,(1,2),i} \\ a'_{k,(2,1),i} & a'_{k,(2,2),i} \end{pmatrix}, \tag{116}$$

$$\overline{\mathbf{R}}_{Ak} = \begin{pmatrix} a'_{k,(1,1),i+1} & a'_{k,(1,2),i+1} \\ a'_{k,(2,1),i+1} & a'_{k,(2,2),i+1} \end{pmatrix}. \tag{117}$$

$a'_{(\cdot)}$ are defined as on page 38. Actually, each block matrix in $\tilde{\mathbf{H}}\tilde{\mathbf{R}}_A\tilde{\mathbf{H}}^H$ contains the information for one user only. From (114), we get

$$\tilde{\mathbf{H}}\tilde{\mathbf{R}}_A\tilde{\mathbf{H}}^H = \sum_{k=1}^{K} [\underline{\mathbf{H}}_k\underline{\mathbf{R}}_{Ak}\underline{\mathbf{H}}_k^H + \mathbf{H}_k\mathbf{R}_{Ak}\mathbf{H}_k^H + \overline{\mathbf{H}}_k\overline{\mathbf{R}}_{Ak}\overline{\mathbf{H}}_k^H] \ . \tag{118}$$

Using $\underline{\mathbf{T}}_{Ak}\dot{\underline{\mathbf{\Lambda}}}_{Ak}\underline{\mathbf{T}}_{Ak}^H$, $\mathbf{T}_{Ak}\dot{\mathbf{\Lambda}}_{Ak}\mathbf{T}_{Ak}^H$, and $\overline{\mathbf{T}}_{Ak}\dot{\overline{\mathbf{\Lambda}}}_{Ak}\overline{\mathbf{T}}_{Ak}^H$ to represent the decompositions of $\underline{\mathbf{R}}_{Ak}$, $\mathbf{R}_{Ak}$, and $\overline{\mathbf{R}}_{Ak}$, respectively, and assuming $\dot{\underline{\mathbf{\Lambda}}}_{Ak}$, $\dot{\mathbf{\Lambda}}_{Ak}$, and $\dot{\overline{\mathbf{\Lambda}}}_{Ak}$ to be the noise free eigenvalues, then under the assumption that the space-time response vectors corresponding to distinct set $\{\theta, \tau\}$ are linearly independent and diagonal character of $\tilde{\mathbf{R}}_A$, we have

$$\tilde{\mathbf{H}}\tilde{\mathbf{R}}_A\tilde{\mathbf{H}}^H = \mathbf{U}_s\dot{\mathbf{\Lambda}}_s\mathbf{U}_s^H \ . \tag{119}$$

In (119), $\underline{\mathbf{H}}_k\underline{\mathbf{R}}_{Ak}\underline{\mathbf{H}}_k^H = \underline{\mathbf{U}}_k\underline{\dot{\mathbf{\Lambda}}}_{Ak}\underline{\mathbf{U}}_k^H$, $\mathbf{H}_k\mathbf{R}_{Ak}\mathbf{H}_k^H = \mathbf{U}_k\dot{\mathbf{\Lambda}}_{Ak}\mathbf{U}_k^H$, and $\overline{\mathbf{H}}_k\overline{\mathbf{R}}_{Ak}\overline{\mathbf{H}}_k^H = \overline{\mathbf{U}}_k\dot{\overline{\mathbf{\Lambda}}}_{Ak}\overline{\mathbf{U}}_k^H$ for $k = 1, ..., K$. With two resolvable paths, $\underline{\dot{\mathbf{\Lambda}}}_{Ak} = [\underline{\dot{\lambda}}_{k,1}\underline{\dot{\lambda}}_{k,2}]$, $\dot{\mathbf{\Lambda}}_{Ak} = [\dot{\lambda}_{k,1}, \dot{\lambda}_{k,2}]$, and $\dot{\overline{\mathbf{\Lambda}}}_{Ak} = [\dot{\overline{\lambda}}_{k,1}, \dot{\overline{\lambda}}_{k,2}]$ contain noise free eigenvalues for kth user. $\overline{\mathbf{U}}_k$, $\mathbf{U}_k$, and $\underline{\mathbf{U}}_k$ are matrices containing the corresponding eigenvectors.

Second step

Pre-multiplying and post-multiplying (119) by $\hat{\mathbf{h}}_{1,l}^H$ and $\hat{\mathbf{h}}_{1,l}$, we have

$$\hat{\mathbf{h}}_{1,l}^H\tilde{\mathbf{H}}\tilde{\mathbf{R}}_A\tilde{\mathbf{H}}^H\hat{\mathbf{h}}_{1,l} = \hat{\mathbf{h}}_{1,l}^H\mathbf{U}_s\dot{\mathbf{\Lambda}}_s\mathbf{U}_s^H\hat{\mathbf{h}}_{1,l} \ , \tag{120}$$

and the following equations are yielded

$$\begin{aligned}
\hat{\mathbf{h}}_{1,l}^H\underline{\mathbf{H}}_k\underline{\mathbf{R}}_{Ak}\underline{\mathbf{H}}_k^H\hat{\mathbf{h}}_{1,l} &= \hat{\mathbf{h}}_{1,l}^H\underline{\mathbf{U}}_k\underline{\dot{\mathbf{\Lambda}}}_{Ak}\underline{\mathbf{U}^H}_k\hat{\mathbf{h}}_{1,l} \ , & (121)\\
\hat{\mathbf{h}}_{1,l}^H\mathbf{H}_k\mathbf{R}_{Ak}\mathbf{H}_k^H\hat{\mathbf{h}}_{1,l} &= \hat{\mathbf{h}}_{1,l}^H\mathbf{U}_k\dot{\mathbf{\Lambda}}_{Ak}\mathbf{U}_k^H\hat{\mathbf{h}}_{1,l} \ , & (122)\\
\hat{\mathbf{h}}_{1,l}^H\overline{\mathbf{H}}_k\overline{\mathbf{R}}_{Ak}\overline{\mathbf{H}}_k^H\hat{\mathbf{h}}_{1,l} &= \hat{\mathbf{h}}_{1,l}^H\overline{\mathbf{U}}_k\dot{\overline{\mathbf{\Lambda}}}_{Ak}\overline{\mathbf{U}^H}_k\hat{\mathbf{h}}_{1,l} \ . & (123)
\end{aligned}$$

Since the eigenvectors span in the signal subspace, we have

$$\begin{aligned}
& |\hat{\mathbf{h}}_{1,l}^H\underline{\mathbf{U}}_1|^2 + |\hat{\mathbf{h}}_{1,l}^H\mathbf{U}_1|^2 + |\hat{\mathbf{h}}_{1,l}^H\overline{\mathbf{U}}_1|^2 + \\
& ... + |\hat{\mathbf{h}}_{1,l}^H\underline{\mathbf{U}}_K|^2 + |\hat{\mathbf{h}}_{1,l}^H\mathbf{U}_K|^2 + |\hat{\mathbf{h}}_{1,l}^H\overline{\mathbf{U}}_K|^2 \qquad (124)\\
= \ & \underline{C}_1 + C_1 + \overline{C}_1 ... + \underline{C}_K + C_K + \overline{C}_K\\
= \ & MN \ ,
\end{aligned}$$

where $0 \leq \underline{C}_k, C_k, \overline{C}_k \leq MN$ for $k = 1, ..., K$. We analyze (121), (122), (123) in three cases at below.

First case For $k \neq 1$, we have $\hat{\mathbf{h}}_{1,l}^H\underline{\mathbf{H}}_k = \mathbf{0}$, $\hat{\mathbf{h}}_{1,l}^H\mathbf{H}_k = \mathbf{0}$, and $\hat{\mathbf{h}}_{1,l}^H\overline{\mathbf{H}}_k = \mathbf{0}$ (by space-time response vectors are linearly independent assumption). Thus, we get

$$|\hat{\mathbf{h}}_{1,l}^H\underline{\mathbf{u}}_{k,1}|^2 = MN\frac{-\underline{\dot{\lambda}}_{k,2}\underline{C}_k}{\underline{\dot{\lambda}}_{k,1} - \underline{\dot{\lambda}}_{k,2}} \ , |\hat{\mathbf{h}}_{1,l}^H\underline{\mathbf{u}}_{k,2}|^2 = MN\frac{\underline{\dot{\lambda}}_{k,1}\underline{C}_k}{\underline{\dot{\lambda}}_{k,1} - \underline{\dot{\lambda}}_{k,2}} \ , \tag{125}$$

$$|\hat{\mathbf{h}}_{1,l}^H\mathbf{u}_{k,1}|^2 = MN\frac{-\dot{\lambda}_{k,2}C_k}{\dot{\lambda}_{k,1} - \dot{\lambda}_{k,2}} \ , |\hat{\mathbf{h}}_{1,l}^H\mathbf{u}_{k,2}|^2 = MN\frac{\dot{\lambda}_{k,1}C_k}{\dot{\lambda}_{k,1} - \dot{\lambda}_{k,1}} \ , \tag{126}$$

$$|\hat{\mathbf{h}}_{1,l}^H\overline{\mathbf{u}}_{k,1}|^2 = MN\frac{-\dot{\overline{\lambda}}_{k,2}\overline{C}_k}{\dot{\overline{\lambda}}_{k,1} - \dot{\overline{\lambda}}_{k,2}} \ , |\hat{\mathbf{h}}_{1,l}^H\overline{\mathbf{u}}_{k,2}|^2 = MN\frac{\dot{\overline{\lambda}}_{k,1}\overline{C}_k}{\dot{\overline{\lambda}}_{k,1} - \dot{\overline{\lambda}}_{k,2}} \ . \tag{127}$$

Because $\underline{\mathbf{R}}_{Ak}$, $\underline{\mathbf{R}}_{Ak}$, and $\underline{\mathbf{R}}_{Ak}$ are positive semidefinite matrices, the eigenvalues are nonnegative. Meanwhile, due to $|\cdot|^2 \geq 0$ in (125) (126) (127), we get $\underline{C}_k = 0$, $C_k = 0$, and $\overline{C}_k = 0$ for $k \neq 1$.

Second case For $k = 1$, we have $\hat{\mathbf{h}}_{1,l}^H\underline{\mathbf{H}}_1 = \mathbf{0}$, and $\hat{\mathbf{h}}_{1,l}^H\overline{\mathbf{H}}_1 = \mathbf{0}$ (by space-time response vectors are linearly independent assumption). Similarly to the first case, we derive $\underline{C}_1 = 0$ and $\overline{C}_1 = 0$. Therefore from (124), we get $C_1 = MN$.

Third case For $k=1$, $\hat{\mathbf{h}}_{1,l}^H \underline{\mathbf{H}}_1 \neq \mathbf{0}$. Utilizing $\hat{\mathbf{h}}_{1,l}^H \mathbf{H}_1 \mathbf{R}_{A1} \mathbf{H}_1^H \hat{\mathbf{h}}_{1,l} = \hat{\mathbf{h}}_{1,l}^H \mathbf{U}_1 \mathbf{\Lambda}_{A1} \mathbf{U}_1^H \hat{\mathbf{h}}_{1,l}$, we derive

$$|\hat{\mathbf{h}}_{1,1}^H \mathbf{u}_{1,l}|^2 = (-1)^l MN \frac{\dot{\lambda}_{1,l'} - MN|E\{a_{1,1,i}\}|^2}{\dot{\lambda}_{1,1} - \dot{\lambda}_{1,2}} \ , \tag{128}$$

$$|\hat{\mathbf{h}}_{1,2}^H \mathbf{u}_{1,l}|^2 = (-1)^l MN \frac{\dot{\lambda}_{1,l'} - MN|E\{a_{1,2,i}\}|^2}{\dot{\lambda}_{1,1} - \dot{\lambda}_{1,2}} \ , \tag{129}$$

where $l^{'} \neq l$. Meanwhile due to $\mathbf{H}_1 \mathbf{R}_{A1} \mathbf{H}_1^H = \mathbf{U}_1 \dot{\mathbf{\Lambda}}_{A1} \mathbf{U}_1^H$, we get

$$\dot{\lambda}_{1,1} + \dot{\lambda}_{1,2} = MN|E\{a_{1,1,i}\}|^2 + MN|E\{a_{1,2,i}\}|^2 \ , \tag{130}$$

$$\dot{\lambda}_{1,1}\dot{\lambda}_{1,2} = (MN)^2 Y \ , \tag{131}$$

where $Y = |E\{a_{1,1,i}\}|^2|E\{a_{1,2,i}\}|^2 - |E\{a_{1,1,i}a_{1,2,i}^*\}|^2$. From the three case analyzed above, only $|\hat{\mathbf{h}}_{1,l}^H \mathbf{u}_{1,1}|^2$ and $|\hat{\mathbf{h}}_{1,l}^H \mathbf{u}_{1,2}|^2$ do not equal to zero.

4.4.2 Performance evaluation for MUSIC

For DOA estimation, general expressions of the mean and variance of MUSIC algorithm in the space array model are derived in [44]. We use $E[\hat{Q}(\theta,\tau)] = \hat{\mathbf{h}}_{1,l}^H \hat{\mathbf{U}}_n \hat{\mathbf{U}}_n^H \hat{\mathbf{h}}_{1,l} = \hat{\mathbf{h}}_{1,l}^H (\mathbf{I} - \hat{\mathbf{U}}_s \hat{\mathbf{U}}_s^H) \hat{\mathbf{h}}_{1,l}$ to present MUSIC algorithm for the two-dimensional code acquisition. Imitating [44], the general expression of the mean of $\hat{Q}(\theta,\tau)$ is derived as

$$\begin{aligned} & E\{\hat{Q}(\theta,\tau)\} \qquad (132) \\ = \ & Q(\theta,\tau) + \frac{\sigma^2}{IX} \sum_{d=1}^{D} \frac{\lambda_d}{(\lambda_d - \sigma^2)^2} [(2NM - D)|\hat{\mathbf{h}}_{1,l}^H \mathbf{u}_d|^2 - Q(\theta,\tau)] + O(\frac{1}{I^2}) \ , \end{aligned}$$

and the general variance of $\hat{Q}(\theta,\tau)$ is derived as

$$Var\{\hat{Q}(\theta,\tau)\} = \frac{2\sigma^2}{I} Q(\theta,\tau) \sum_{d=1}^{D} \frac{\lambda_d}{(\lambda_d - \sigma^2)^2} |\hat{\mathbf{h}}_{1,l}^H \mathbf{u}_d|^2 + O(\frac{1}{I^2}) \ . \tag{133}$$

With the assumption that the space-time response vectors corresponding to distinct set $\{\theta,\tau\}$ are linearly independent, for the special case that each user has two resolvable paths, the mean of (132) in the directions of $\{\theta_{1,1},\tau_{1,1}\}$ and $\{\theta_{1,2},\tau_{1,2}\}$ can be obtained as

$$\begin{aligned} E\{\hat{Q}(\theta,\tau)\} \ = \ & Q(\theta,\tau) + \frac{\sigma^2(2NM - D)}{IX} [\frac{\sigma^2}{MNY} + \frac{E\{|a_{1,l',i}\}|^2}{Y} \qquad (134) \\ - \ & \frac{\sigma^2(|E\{a_{1,1,i}\}|^2 + |E\{a_{1,2,i}\}|^2)|E\{a_{1,l',i}\}|^2}{MNY^2}] + O(\frac{1}{I^2}) \ . \end{aligned}$$

The bias is

$$\begin{aligned} \eta \ = \ & \frac{\sigma^2(2NM - D)}{IX} [\frac{\sigma^2}{MNY} + \frac{|E\{a_{1,l',i}\}|^2}{Y} \qquad (135) \\ - \ & \frac{\sigma^2(|E\{a_{1,1,i}\}|^2 + |E\{a_{1,2,i}\}|^2)|E\{a_{1,l',i}\}|^2}{MNY^2}] + O(\frac{1}{I^2}) \end{aligned}$$

and the variance of (133) is

$$Var\{\hat{Q}(\theta,\tau)\} = \frac{2\sigma^2}{I}Q(\theta,\tau)[\frac{\sigma^2}{MNY}+\frac{|E\{a_{1,l',i}\}|^2}{Y} - \frac{\sigma^2(|E\{a_{1,1,i}\}|^2+|E\{a_{1,2,i}\}|^2)|E\{a_{1,l',i}\}|^2}{MNY^2}]+O(\frac{1}{I^2}) \ , \quad (136)$$

where $l \neq l^{'}$. The goal for accurate parameter estimation is to mitigate η. (132) shows that the degradation of η can be achieved by enlarging I, X, Y, and MN. Here MN is defined as the length of a space-time response vector. Due to the high-correlation/coherency, Y turns to small. This results in η to be higher. In [44], $X = 1$ in (111) for MUSIC algorithm, and $X = 2$ is derived as using the one forward-backward smoothing to mitigate the huge bias caused by two coherent sources in the space array model. Distinguish to [44] enlarging X, the derived asymptotic statistical properties show that the length of space-time response vector can be considered for mitigating the huge bias caused by high-correlation/coherency in the DS-CDMA array model. Since the processing gain N is as denumerate in (135), a further performance improvement is given with the increasing N. One can see from (135) that the first and third terms have a N degradation. Meanwhile form (136), we see $Var\{\hat{Q}(\theta,\tau)\}$ is zero within a first order approximation.

Numerical experiments

Some numerical examples illustrate the MUSIC algorithm for two-dimensional code acquisition in an asynchronous DS-CDMA uplink channel where the received multi-user signals undergo frequency selective Rayleigh fading.

For each simulation, only the code of the first user is known. Any parameters, such as time-varying attenuation factors, are assumed to be unknown. Gold codes of length $N = 15$ and $N = 31$ are used for spreading. A uniform linear array with a half wavelength element spacing is used. Time delays are assumed discrete and uniformly distributed over $[0, 0.1, ..., 12]$ chips for $N = 15$ and $[0, 0.1, ..., 21]$ chips for $N = 31$. The angle spread is within a span of 60°. The number of users K is set as 1 and 5 respectively, and the number of resolvable paths is $L = 2$. The total number of source signals is $3KL$. Due to the limited information that only the number of incident signals is known, the signal subspace dimension is defined $D = 3KL$, even for coherent multipath propagation. We assume $\tau_{1,1} < \tau_{1,2}$. All simulation results are based on 1000 independent runs.

The parameters $\{\theta_{1,1}, \tau_{1,1}\}$ and $\{\theta_{1,2}, \tau_{1,2}\}$ are estimated by picking the two largest values from a two-dimensional searching spectrum. A successful acquisition is regarded when the estimation error of the time delay is less than half a chip duration, and the estimation error of DOA is less than 3°. With a successful acquisition, the estimation accuracy is measured using the root mean-square error (RMSE). In this thesis, RMSE for time delay and DOA are given respectively

as

$$RMSE_\tau = \sqrt{E[(\hat{\tau}-\tau)^2]|(|\hat{\tau}-\tau| \leq T_c/2)} \ , \quad (137)$$
$$RMSE_\theta = \sqrt{E[(\hat{\theta}-\theta)^2]|(|\hat{\theta}-\theta| \leq 3^o)} \ .$$

Tables 1 and 2 list the probabilities of a successful time delay acquisition for the first and second paths. Tables 3 and 4 list the probabilities of a successful DOA acquisition for the first and second paths respectively. Generally, the estimation performance of MUSIC is increased with large SNR or symbol collection. Because the much longer processing gain causes a much stronger assumption of linear independence, here we mainly examine the effect of the space-time response vector's length for successful parameter acquisition. In the set of simulations, we fix M as 10, and chose N as 15 and 31 respectively. Such, the length of space-time response vectors are 150 for $N = 15$, and 310 for $N = 31$. In the tables, the average SNRs are chosen as 0dB, 10dB, and 20dB. In $K = 5$ case, all the interfering users have the same energy as for the desired user. Meanwhile, we set each user an equal-energy two-path Rayleigh fading channel, and $I = 200$. The correlation coefficients $\rho_{k(l,l')}$ between two paths for each user are set at the same value. In this thesis, four distinct values $\rho_{k(l,l')} = 0, 0.5, 0.8, 1$ are examined. The first thing that stands out from the tables is that the achieved probabilities of acquisition for the five users case are quite the same as the one user case when $N = 31$ for the four correlation relationships. However, when $N = 15$, the probabilities of a successful acquisition for the five users case are lower compared to the one user case. The phenomenon tells that the large value of N causes the linear independence of space-time response vectors to be a stronger assumption. Hence, as the parameters are estimated in a two-dimensional spectrum, interfering users are shielded away. In this case, the system turns to be no MAI, in other words, a one user system. Meanwhile, here we note that $2NM - D$ is proportional to N as D is fixed. The bias in (135) may go up by increasing N, hence one can see from the tables that the achieved probabilities of acquisition for $N = 31$ are lower than for $N = 15$ in case of $SNR = 0dB$ and $K = 1$ situation. The second thing stands out that high probabilities of a successful acquisition are given for the high-correlated/coherent two paths transmission. Compared to uncorrelated two paths transmission, tables I and II shows that the probability of correct time delay acquisition for coherent two paths only has 1.5% degradation as $N = 31$ and $SNR = 20dB$. However when $N = 15$ and $SNR = 20dB$, it has more than 10% reduction. The probabilities of correct DOA acquisition in tables III and IV have the similar scene. It is hence expected that with a large value of space-time response vector length, the performance of MUSIC is greatly improved.

In Figs 4-7, RMSEs are plotted as a function of varying Signal-to-Noise Ratio (SNR) which is from 0dB to 20dB in increments of 2dB. The inspections of accuracy for two-dimensional code acquisition are performed in four distinct correlation relationships. As can be seen from the figures, MUSIC always provides accurate DOA and time delay estimation when $N = 31$. Due to the time interval

TABLE 1 Probabilities of successful time delay acquisition for the first path. Each user has an equal-energy two-path Rayleigh fading channel. $I = 200$, $M = 10$, $D = 3KL$. The average $SNR = 0, 10, 20dB$. As $K = 5$ case, $MAI = 0dB$.

K		1			5		
SNR		0	10	20	0	10	20
$\rho_{k(l,l')} = 0$,	$N = 15$	86.6	100	100	50.8	84.6	90.0
	$N = 31$	60.0	100	100	66.0	99.3	99.3
$\rho_{k(l,l')} = 0.5$	$N = 15$	81.0	100	100	48.4	82.4	89.8
	$N = 31$	58.0	100	100	64.0	99.3	99.3
$\rho_{k(l,l')} = 0.8$	$N = 15$	72.4	100	100	40.4	72.6	89.4
	$N = 31$	62.0	99.7	100	60.0	98.3	99.3
$\rho_{k(l,l')} = 1$	$N = 15$	75.8	86.8	100	40.8	42.4	77.8
	$N = 31$	69.7	77.7	100	68.7	81.7	97.7

TABLE 2 Probabilities of successful time delay acquisition for the second path. Each user has an equal-energy two-path Rayleigh fading channel. $I = 200$, $M = 10$, $D = 3KL$. The average $SNR = 0, 10, 20dB$. As $K = 5$ case, $MAI = 0dB$.

K		1			5		
SNR		0	10	20	0	10	20
$\rho_{k(l,l')} = 0$	$N = 15$	82.6	100	100	45.2	81.0	89.6
	$N = 31$	53.3	99.7	100	65.3	99.7	99.7
$\rho_{k(l,l')} = 0.5$	$N = 15$	77.8	100	100	42.4	79.6	89.0
	$N = 31$	57.0	99.7	100	60.0	99.3	99.7
$\rho_{k(l,l')} = 0.8$	$N = 15$	73.2	99.8	100	39.4	71.0	89.0
	$N = 31$	66.0	98.3	100	58.3	95.7	99.7
$\rho_{k(l,l')} = 1$	$N = 15$	78.4	88.6	100	39.6	41.6	78.8
	$N = 31$	72.3	80.0	100	66.3	78.7	98.3

TABLE 3 Probabilities of successful DOA acquisition for the first path. Each user has an equal-energy two-path Rayleigh fading channel. $I = 200$, $M = 10$, $D = 3KL$.The average $SNR = 0, 10, 20dB$. As $K = 5$ case, $MAI = 0dB$.

K		1			5		
SNR		0	10	20	0	10	20
$\rho_{k(l,l')} = 0$	$N = 15$	92.4	100	100	51.8	85.4	91.8
	$N = 31$	74.7	100	100	78.0	100	100
$\rho_{k(l,l')} = 0.5$	$N = 15$	87.7	100	100	48.2	82.8	91.4
	$N = 31$	72.3	100	100	76.0	100	100
$\rho_{k(l,l')} = 0.8$	$N = 15$	79.6	100	100	43.6	77.4	90.4
	$N = 31$	72.6	99.7	100	72.7	100	100
$\rho_{k(l,l')} = 1$	$N = 15$	83.0	91.6	100	45.4	46.6	80.6
	$N = 31$	79.0	86.0	100	81.0	90.3	99.0

TABLE 4 Probabilities of successful DOA acquisition for the second path. Each user has an equal-energy two-path Rayleigh fading channel. $I = 200$, $M = 10$, $D = 3KL$. The average $SNR = 0, 10, 20dB$. As $K = 5$ case, $MAI = 0dB$.

K		1			5		
SNR		0	10	10	0	10	20
$\rho_{k(l,l')} = 0$	$N = 15$	88.4	100	100	48.6	83.6	91.4
	$N = 31$	68.7	100	100	75.7	100	100
$\rho_{k(l,l')} = 0.5$	$N = 15$	86.0	100	100	45.6	82.2	90.8
	$N = 31$	73.0	100	100	74.7	99.7	100
$\rho_{k(l,l')} = 0.8$	$N = 15$	82.8	99.8	100	43.4	72.2	91.2
	$N = 31$	78.7	99.0	100	75.0	98.0	100
$\rho_{k(l,l')} = 1$	$N = 15$	86.4	93.6	100	47.6	50.8	81.0
	$N = 31$	85.7	90.7	100	79.3	84.7	99.3

$T_c/2$ is set in the two-dimensional searching spectrum, the great enhancement of accuracy estimation for time delay can not be seen as $N = 31$ in the coherent multipath propagation environment.

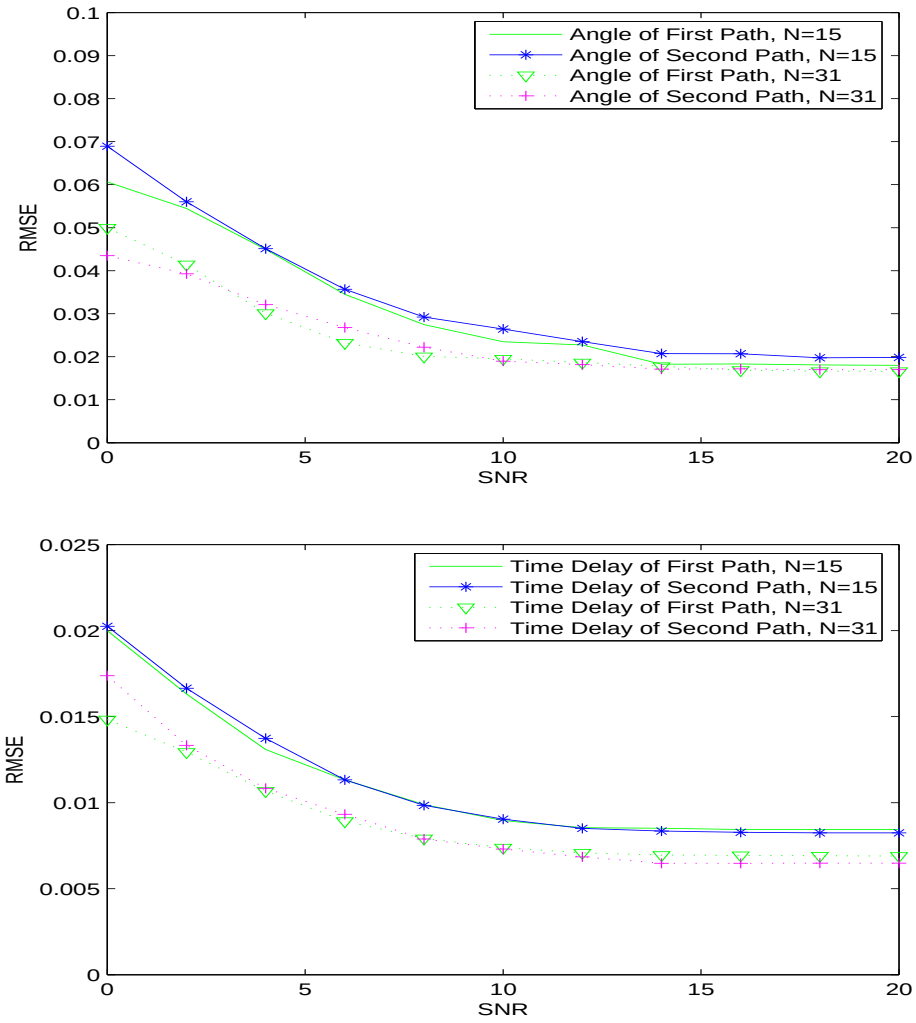

FIGURE 4 RMSE as a function of Signal-to-Noise (SNR) in an equal energy two-path Rayleigh fading channel. There are $K = 5$ users. Symbols number is chosen as 200. The number of antenna sensors is 10. All the interfering users have equal energy as the desired user. The signal subspace $D = 3KL$. The correlation coefficients $\rho_{k(l,l')}$ between two paths for each user are set same value. $\rho_{STV-k(l,l')} = 0$.

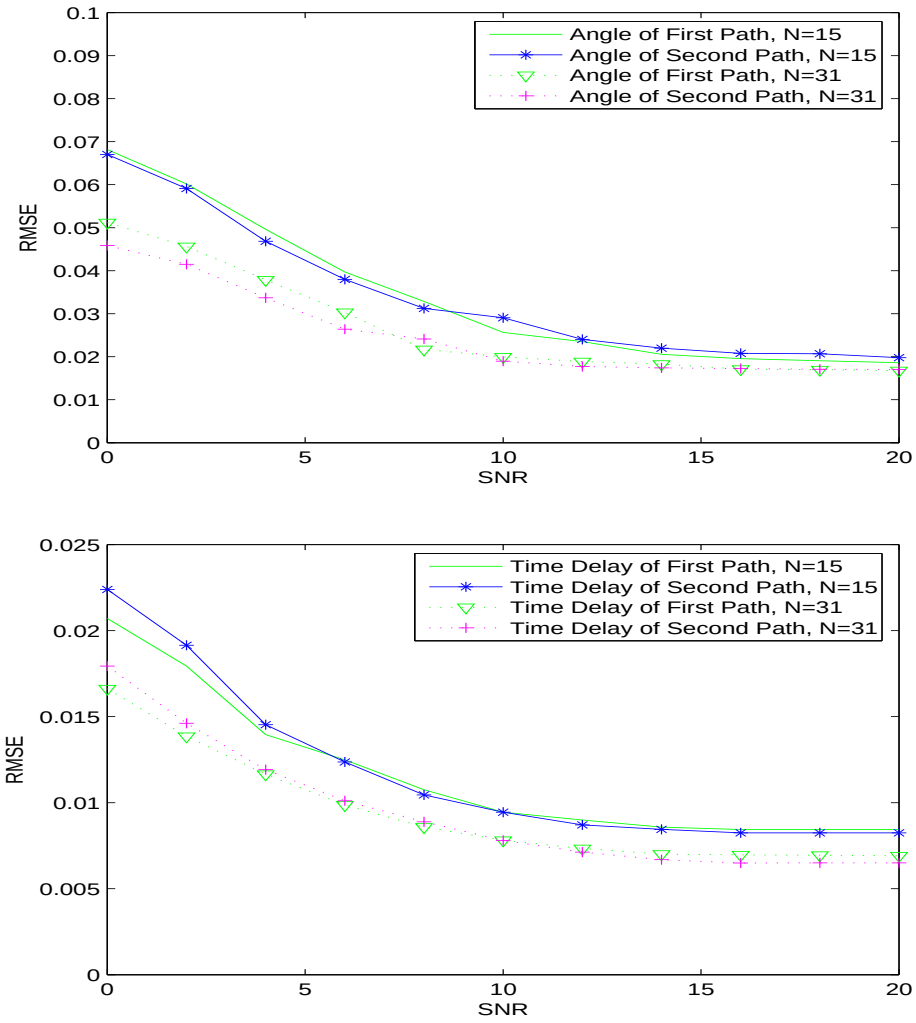

FIGURE 5 RMSE as a function of Signal-to-Noise (SNR) in an equal energy two-path Rayleigh fading channel. There are $K = 5$ users. Symbols number is chosen as 200. The number of antenna sensors is 10. All the interfering users have equal energy as the desired user. The signal subspace $D = 3KL$. The correlation coefficients $\rho_{k(l,l')}$ between two paths for each user are set same value. $\rho_{STV-k(l,l')} = 0.5$.

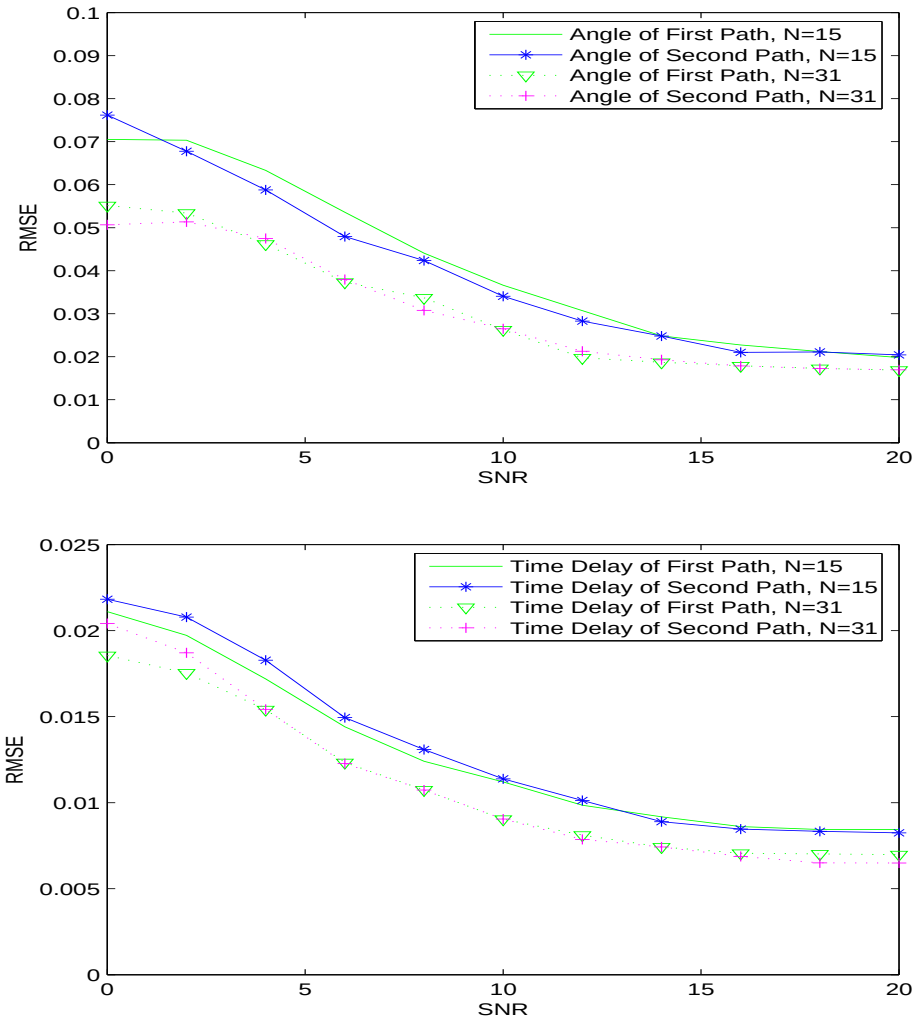

FIGURE 6 RMSE as a function of Signal-to-Noise (SNR) in an equal energy two-path Rayleigh fading channel. There are $K = 5$ users. Symbols number is chosen as 200. The number of antenna sensors is 10. All the interfering users have equal energy as the desired user. The signal subspace $D = 3KL$. The correlation coefficients $\rho_{k(l,l')}$ between two paths for each user are set same value. $\rho_{STV-k(l,l')} = 0.8$.

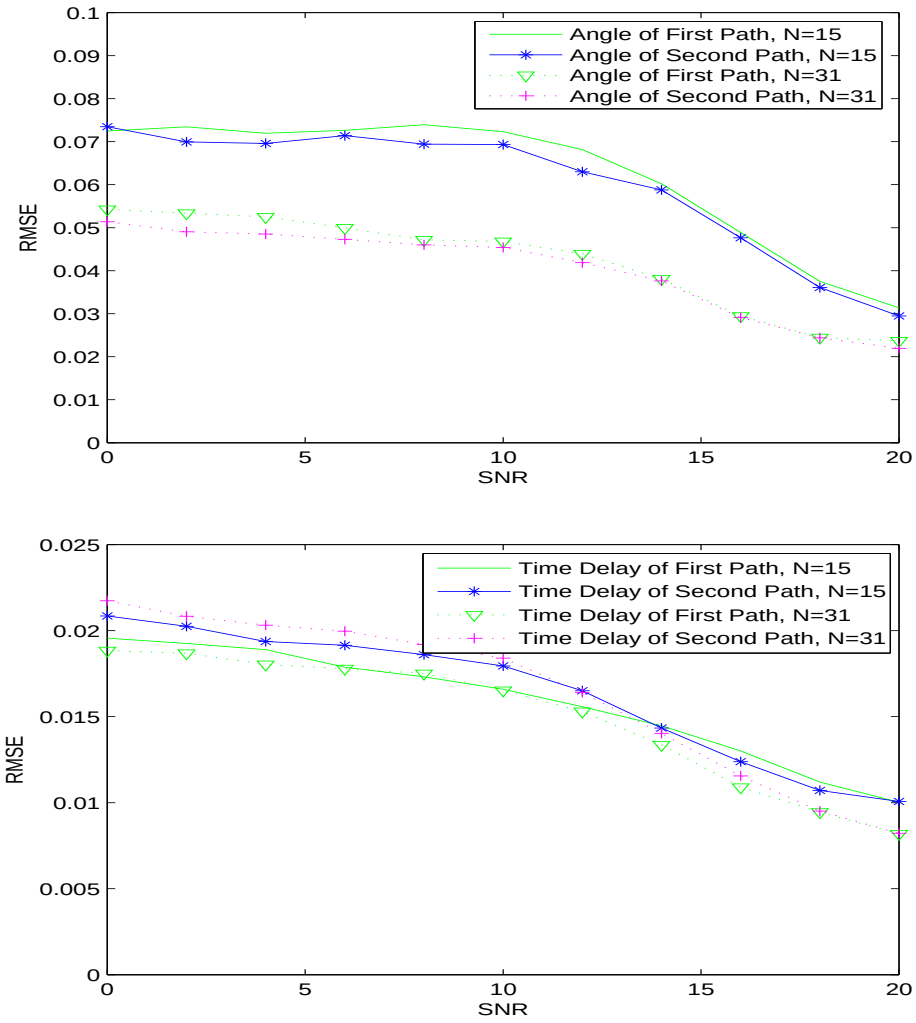

FIGURE 7 RMSE as a function of Signal-to-Noise (SNR) in an equal energy two-path Rayleigh fading channel. There are $K = 5$ users. Symbols number is chosen as 200. The number of antenna sensors is 10. All the interfering users have equal energy as the desired user. The signal subspace $D = 3KL$. The correlation coefficients $\rho_{k(l,l')}$ between two paths for each user are set same value. $\rho_{STV-k(l,l')} = 1$.

5 CONCLUSIONS

In this thesis, we present parametric algorithms to estimate the channel parameter in wireless communication systems. The focus is on the two-dimensional code acquisition in DS-CDMA array model, and two main categorial algorithms are developed.

The first is a semi-blind method based algorithm called ICA. The main benefit of applying ICA for two-dimensional code acquisition is its capability to combat the MAI problem. To handle a non-stationary environment, e.g. the case of a fading channel, ICA is further developed. A pre-processing operation is performed in frequency domain to pre-suppress interferences before applying ICA for two-dimensional code acquisition. In this case, a further benefit, which parameter estimation can be performed in the fading channel, is provided.

The second is a subspace based method called EV-t. EV-t looks for a maximum projection of the desired signal's space-time direction on the signal subspace and searches the training sequence support which is assumed to be available. As EV-t is exploited for two-dimensional code acquisition, its advantage is that the two-dimensional code acquisition can be performed in the high-correlated/coherent multipath propagation environment regardless the correlation between the various paths from the same user, and the parameter estimation is performed with small received sets of samples in the high MAI environment.

Furthermore, this thesis analyzes the asymptotic statistical properties of MUSIC in the special case that each user has two resolvable paths, and the analysis is based on the assumption that the space-time response vectors corresponding to distinct set $\{\theta, \tau\}$ are linearly independent.

Based on the DS-CDMA array model, this thesis provides efficient algorithms for two-dimensional code acquisition. However, two -dimensional code acquisition needs two dimensional search, the reduction in computational cost is our next task.

APPENDIX 1

In DS-CDMA systems, the spreading code assigned to different users have special properties. With the assumption of a narrow auto-correlation for each user's spreading code vector, the autocorrelation coefficients can be designed as [23]

$$\underline{\rho}_{CV-k(l,l')} = \underline{\mathbf{c}}_{k,l}^{T}(\tau_{k,l})\underline{\mathbf{c}}_{k,l'} = \begin{cases} \tau_{k,l} \ , & |\tau_{k,l} - \tau_{k,l'}| = 0 \ , \\ \approx \sqrt{\tau_{k,l}} \ , & |\tau_{k,l} - \tau_{k,l'}| > T_c \ . \end{cases} \tag{138}$$

$$\rho_{CV-k(l,l')} = \mathbf{c}_{k,l}^{T}(\tau_{k,l})\mathbf{c}_{k,l'} = \begin{cases} N \ , & \tau_{k,l} - \tau_{k,l'} = 0 \ , \\ \approx \sqrt{N} \ , & |\tau_{k,l} - \tau_{k,l'}| > T_c \ . \end{cases} \tag{139}$$

$$\overline{\rho}_{CV-k(l,l')} = \overline{\mathbf{c}}_{k,l}^{T}(\tau_{k,l})\overline{\mathbf{c}}_{k,l'} = \begin{cases} N - \tau_{k,l} \ , & |\tau_{k,l} - \tau_{k,l'}| = 0 \ , \\ \approx \sqrt{N - \tau_{k,l}} \ , & |\tau_{k,l} - \tau_{k,l'}| > T_c \ . \end{cases} \tag{140}$$

Also the low cross-correlations for different users's spreading code vectors have the expression as

$$\underline{\rho}_{CV-(k,k')(l,l')} = \underline{\mathbf{c}}_{k,l}^{T}(\tau_{k,l})\underline{\mathbf{c}}_{k,l'}(\tau_{k',l'}) = \begin{cases} 0 \ , & |\tau_{k,l} - \tau_{k',l'}| = 0 \ , \\ \approx \sqrt{\tau_{k,l}} \ , & |\tau_{k,l} - \tau_{k',l'}| > T_c \ . \end{cases} \tag{141}$$

$$\rho_{CV-(k,k')(l,l')} = \mathbf{c}_{k,l}^{T}(\tau_{k,l})\mathbf{c}_{k',l'} = \begin{cases} 0 \ , & |\tau_{k,l} - \tau_{k',l'}| = 0 \ , \\ \approx \sqrt{N} \ , & |\tau_{k,l} - \tau_{k',l'}| > T_c \ . \end{cases} \tag{142}$$

$$\overline{\rho}_{CV-(k,k')(l,l')} = \overline{\mathbf{c}}_{k,l}^{T}(\tau_{k,l})\overline{\mathbf{c}}_{k',l'} = \begin{cases} 0 \ , & |\tau_{k,l} - \tau_{k',l'}| = 0 \ , \\ \approx \sqrt{N - \tau_{k,l}} \ , & |\tau_{k,l} - \tau_{k',l'}| > T_c \ . \end{cases} \tag{143}$$

Due to $\underline{\mathbf{c}}_{k,l}$, $\mathbf{c}_{k,l}$, and $\overline{\mathbf{c}}_{k,l}$ are the "previous", "current", and the "next" code vectors, the correlation coefficients of $\underline{\mathbf{c}}_{k,l}^{T}(\tau_{k,l})\mathbf{c}_{k',l'} \approx 0$ and $\underline{\mathbf{c}}_{k,l}^{T}(\tau_{k,l})\overline{\mathbf{c}}_{k',l'} \approx 0$ for $k, k^{'} = 1, ..., K$ and $l, l^{'} = 1, ..., L$.

Generally, the linearly independent assumption of array response vectors corresponding to distinct value θ are widely accepted. As it is a weak assumption, a reasonable consideration that low correlation coefficient, e.g. ρ_s, exist between two array response vectors with different θ. In this case, the auto-correlation coefficients of space-time response vectors $\rho_{STV-k(l,l')}$ are as

$$\underline{\rho}_{STV-k(l,l')} = \underline{\mathbf{h}}_{k,l}^{H}\underline{\mathbf{h}}_{k,l'} = \begin{cases} \tau_{k,l} \ , \rho_s & |\tau_{k,l} - \tau_{k,l'}| = 0 \ , \\ \approx \sqrt{\tau_{k,l}}\rho_s \ , & |\tau_{k,l} - \tau_{k,l'}| > T_c \ . \end{cases} \tag{144}$$

$$\rho_{STV-k(l,l')} = \mathbf{h}_{k,l}^{H}\mathbf{h}_{k,l'} = \begin{cases} N\rho_s \ , & |\tau_{k,l} - \tau_{k,l'}| = 0 \ , \\ \approx \sqrt{N}\rho_s \ , & |\tau_{k,l} - \tau_{k,l'}| > T_c \ . \end{cases} \tag{145}$$

$$\overline{\rho}_{STV-k(l,l')} = \overline{\mathbf{h}}_{k,l}^{H}\overline{\mathbf{h}}_{k,l'} = \begin{cases} (N-\tau_{k,l})\rho_s \ , & |\tau_{k,l}-\tau_{k,l'}| = 0 \ , \\ \approx \sqrt{N-\tau_{k,l}}\rho_s \ , & |\tau_{k,l}-\tau_{k,l'}| > T_c \ . \end{cases} \quad (146)$$

As $|\tau_{k,l} - \tau_{k,l'}| = 0$, the auto-correlation coefficients of the space-time response vector are the same as the correlation coefficients of the array response vectors. However, if $|\tau_{k,l} - \tau_{k,l'}| > T_c$, the auto-correlation coefficients of the space-time response vectors have a $\sqrt{\cdot}$ reduction compared to the correlation coefficients of the array response vectors.

The cross-correlation coefficients of space-time response vectors are

$$\underline{\rho}_{STV-(k,k')(l,l')} = \underline{\mathbf{h}}_{k,l}^{H}\underline{\mathbf{h}}_{k',l'} = \begin{cases} 0 \ , & |\tau_{k,l}-\tau_{k',l'}| = 0 \ , \\ \approx \sqrt{\tau_{k,l}}\rho_s \ , & |\tau_{k,l}-\tau_{k',l'}| > T_c \ . \end{cases} \quad (147)$$

$$\rho_{STV-(k,k')(l,l')} = \mathbf{h}_{k,l}^{H}\mathbf{h}_{k',l'} = \begin{cases} 0 \ , & |\tau_{k,l}-\tau_{k',l'}| = 0 \ , \\ \approx \sqrt{N}\rho_s \ , & |\tau_{k,l}-\tau_{k',l'}| > T_c \ . \end{cases} \quad (148)$$

$$\overline{\rho}_{STV-(k,k')(l,l')} = \overline{\mathbf{h}}_{k,l}^{H}\overline{\mathbf{h}}_{k',l'} = \begin{cases} 0 \ , & |\tau_{k,l}-\tau_{k',l'}| = 0 \ , \\ \approx \sqrt{N-\tau_{k,l}}\rho_s \ , & |\tau_{k,l}-\tau_{k',l'}| > T_c \ . \end{cases} \quad (149)$$

As $|\tau_{k,l} - \tau_{k,l'}| = 0$, the cross-correlation coefficients of the space-time response vectors equal to zeros. For the case of $|\tau_{k,l} - \tau_{k,l'}| > T_c$, the cross-correlation coefficients of the space-time response vectors decrease $\frac{1}{\sqrt{\cdot}}$ order compared to the correlation coefficients of the array response vectors.

In the space array model, the linearly independent assumption of array response vectors corresponding to different values θ are widely accepted. For distinct set $\{\theta, \tau\}$, we can say that the linearly independent assumption of the space-time response vectors is more stronger than that of the array response vectors.

REFERENCES

[1] J. S. Blogh, L. Hanzo, "Third Gneration Systems and Intelligent Wireless Networking: Smart Antennas and Adaptive Modulation", John Wiley and Sons Inc., New York, 2002.

[2] W. R. Braun, U. Dersch, "A Physical Mobile Radio Channel Model", IEEE Trans. on Vehicular Technology, vol. 40, pp. 472-482, May 1991.

[3] A. Cicho, S. Amari, "Adaptive Blind Signal and Image Processing", John Wiley and Sons, West Sussex, UK, 2002.

[4] A.D. Back, A.C. Tsoi, "Blind deconvolution of signals using a complex recurrent network", Neural Networks for Signal processing [1994] IV. Proceedings of the 1994 IEEE Workshop, Ermioni, Greece, pp. 565-574, Sep. 1994.

[5] A.J. Barabell, "Improving the resolution performance of eigenstructure based direction finding algorithms", Proc. IEEE ICASSP, Boston, MA, pp. 336-339, 1983.

[6] S.E. Bensley, B. Aazhang, "Subspace-based channel estimation for code division multiple access communication systems", IEEE Trans. on Communications, vol. 44, pp. 1009 -1020, Aug. 1996.

[7] E. Bingham, A. Hyvärinen, "A fast fixed-point algorithm for independent component analysis of complex valued signals", International Journal of Neural Systems, vol. 10, pp. 1-8, Feb. 2000.

[8] J. Capon, "High resolution frequency-wavenumber spectral analysis", Proceedings of the IEEE, vol. 57, pp. 1408-1418, Aug. 1969.

[9] R. Cristescu, J. Joutsensalo, and T. Ristaniemi, "Fading channel estimation by mutual information minimization for Gaussian stochastic processes", Proc. IEEE International Conference on Communications (ICC 2000), New Orleans, USA, pp. 56-59, Jun. 2000.

[10] R. Cristescu, J. Joutsensalo, T. Ristaniemi, and J. Karhunen, "Delay estimation in CDMA communications using a FastICA algorithm", Proc. International Workshop on Independent Component Analysis and Signl Separation (ICA), Helsinki, Finland, pp. 105-110, Jun. 2000.

[11] R. Cristescu, J. Joutsensalo, T. Ristaniemi, and J. Karhunen, "Blind Separation of convolved mixtures for CDMA systems", Proc. European Signal Processing Conference (EUSIPCO), Tampere, Finland, CD-ROM, Sep. 2000.

[12] R. Cristescu, J. Joutsensalo, T. Ristaniemi, and J. Karhunen,"CDMA delay estimation using FastICA algorithm", Proc. The 11th IEEE International Symposium on Personal, Indoor, and Mobile Radio Communications (PIMRC), London, pp. 1117-1120, Sep. 2000.

[13] S.E. Fienberg, D.V. Hinkley, "R.A. Fisher: An application", Lecture Notes in Statistics, Spinger-Verlag, New York, 1990.

[14] L. C. Godara, "Applications of Antenna Arrays to Mobile Communications, part I: Performance Improvement, feasibility, and System Considerations", Procedings of the IEEE, vol. 85, pp. 1031-1060 , July 1997.

[15] Z. Gu, E. Gunawan, "Joint space-time estimation for DS-CDMA system in fast fading multipath channel", IEEE Electronics Letters, vol. 37, pp. 1407-1408, Nov. 2001.

[16] D. Hösli, "Spatial-Temporal Short-Code CDMA-systems", MSc thesis, Imperial College, 2001.

[17] L.H. Huang, A. Manikas, "Blind adaptive single-user array receiver for MAI cancellation in multipath", Proc. European Signal Processing Conference (EUSIPCO), vol. 2, pp. 647-650, Sep. 2000.

[18] A. Hyvarinen, E. Oja, "A fast fixed-point algorithm for independent component analysis", Neural Computation, vol. 9, pp. 1483-1492, 1997.

[19] A. Hyvarinen, J. Karhunen, and E.Oja, "Independent Component Analysis", John Wiley & Sons, New York, 2001.

[20] W.C. Jakes, "Microwave mobile communications", John Wiley & Sons, New York, 1974.

[21] D.H. Johnson, S. Degraaf, "Improving the Resolution of Bearing in Passive Sonar Arrays by Eigenvalue analysis", IEEE Trans. on Signal Processing, vol. 30, pp.638-647, Aug. 1982.

[22] M. Kaveh, A. Barabell, "The statistical performance of the MUSIC and the minimum-norm algorithms in resolving plane waves in noise", IEEE Trans. on Acoustics, Speech, and Signal Processing, vol. 34, pp. 331-341, Apr. 1986.

[23] B. H. Khalaj, A. Paulraj, and T. Kailath, "2D RAKE Receivers for CDMA Cellular Systems", Proc. IEEE Global Telecommunications Conference, pp. 400-404, Dec. 1994.

[24] J. Kiefer, J. Wolfowitz, "Consistency of the maximum likelihood estimator in the presence of infinitinely many incidental parameters", The Annals of Mathematical Statistics, vol. 27, pp. 887-906, 1956.

[25] E. Kreyszig, "Advanced Engineering Mathematics", John Wiley, New York, 1983.

H. Krim, M. Viberg, "Two decades of array signal processing research: the parametric approach", IEEE Signal Processing Magazine, vol. 13, pp. 67-94, Jul. 1996.

[26] R. Kumaresan, D.W. Tufts, "Estimating the angle of arrival of multiple plane waves", IEEE Trans. on Aerospace and Electronic Systems, vol. 19, pp. 134-139, Jan. 1983.

[27] E. Lindskog, A. Ahlen, and M. Sternad, "Spatio-temporal equalization for multipath environments in mobile radio applications", Proc. IEEE Vehicular Technology Conference, vol. 1, pp. 399-403, Jul. 1995.

[28] J. Litva, T.K.-Y. Lo, "Digital Beamforming in Wireless Communications", Artech House, Boston, 1996.

[29] A. Manikas, M. Sethi, "A Space-Time Channel Estimatin and Single-User Receiver for Code-Resue DS-CDMA Systems," IEEE Trans. on Signal Processing, vol. 51, pp. 39-51, Jan. 2003.

[30] E. Moreau, O. Macchi, "Complex self-adaptive algorithms for source separation based on high order contrasts", Proc. VII European Signal Processing Conference, Edinburgh, Scotland, vol. 2, pp. 1157-1160, Sep. 1994.

[31] J. W. Modestino, V. M. Eyuboglu, "Integrated multielement receiver structures for spatially distributed interference channels", Trans. on Information Theory, vol. 32, pp. 195-219, Mar. 1986.

[32] Okamoto, T. Garret, "Smart Antenna Systems and wirelss Lans", New York, Kluwer Academic Publishers, 2002.

[33] B. Ottersten, M. Viberg, "Asymptotic results for multidimensional sensor array processing", The 22th Annular Asilomar Conference on Signals, Systems and Computers, Monterey, USA, pp. 833-837, 1988.

[34] B. Ottersten, "Parametric subspace fitting methods for array signal processing", Ph.D. thesis, Stanford University, USA, 1990.

[35] B. Ottersten, M. Viberg, and T. Kailath, "Performance analysis of the total least squares ESPRIT algorithm", IEEE Trans. on Signal Processing, vol. 39, pp. 1122-1135, May 1991.

[36] B. Ottersten, M. Viberg, and T. Kailath, "Analysis of subspace fitting and ML techniques for parameter estimation from sensor array data", IEEE Trans. on Signal Processing, vol. 40, pp. 590-599, Mar. 1992.

[37] B. Ottersten, M. Viberg, P. Stoica, and A, Nehorai, "Exact and large sample maximum likelihood techniques for parameter estimation and detection in array processing", Radar Array Processing, Springer-Verlag, Berlin, Chap. 4, pp.99-151, 1993.

[38] S. Parkvall, "Near-far resistant DS-CDMA systems: parameter estimation and data detection", PhD thesis, Royal Institute of Technology, KTH, Stockholm, Sweden, 1996.

[39] S. Parkvall, E. Strom, and B. Ottersten, "The impact of timing errors on the performance of linear DS-CDMA receiver", IEEE Journal on selected Areas in Communication, vol. 14, pp. 1660-1668, Oct. 1996.

[40] A. Paulraj, R. Roy, and T. Kailath, "A subspace rotation approach to signal parameter estimation", Proceedings of IEEE, vol. 74, pp. 1044-1045, Jul. 1986.

[41] A. Paulraj, "Space-Time Processing for Wireless Communications", IEEE Signal Processing Magazine, vol. 14, pp. 49-83, Nov. 1997.

[42] R. Peterson, R. Ziemer, and Borth D, "Introduction to Spread Spectrum Communications", Prentice Hall, Englewood Cliff, New Jersey, 1995.

[43] S.U. Pillai, B.H. Kwon, "Forward/backward spatial smoothing techniques for coherent signal identification", IEEE Trans. on Acoustics, Speech, and Signal Processing, vol. 37, pp. 8-15, Jan. 1989.

[44] S.U. Pillai, "Array Signal Processing", Springer-Verlag, New York, 1989.

[45] B. Porat, B. Friedlander, "Analysis of the asymptotic relative efficiency of the MUSIC algorithm", IEEE Trans. on Acoustics, Speech, and Signal Processing, vol. 36, pp. 532-544, Apr. 1988.

[46] R. Price, P.E. Green, "A communication technique for the multipath channels", Proceedings of the IRE, vol. 46, pp. 555-569, Mar. 1958.

[47] J.G. Proakis, "Digital communication", 2nd ed., McGraw-Hill, New York, 1989.

[48] G.G. Raleigh, T. Boros, "Joint space-time parameter estimation for wireless communication channels", IEEE Trans. on Signal Processing, vol. 46, pp. 1333-1343, May 1998.

[49] T.S. Rappaport, "Wireless communications: principles and practice", Prentice-Hall, Englewood Cliffs, New Jersey, 1996.

[50] S.S. Reddi, "Multiple source location - a digital approach", IEEE Trans. on Aerospace and Electronic Systems, vol. 15, pp. 95-105, 1979.

[51] T. Ristaniemi, J. Joutsensalo, "On the performance of blind source separation in CDMA donwlink", Proc. International Workshop on Independent Component Analysis and Signal Separation, (ICA'99), Aussois, France, pp. 437-442, Jan. 1999.

[52] T. Ristaniemi, J. Joutsensalo, "Independent component analysis with code information utilization in DS-CDMA signal separation", Proc. IEEE GLOBECOM, Rio de Janeiro, Brazil, pp. 320-324, Dec. 1999.

[53] T. Ristaniemi, J. Joutsensalo, "Advanced ICA-based receivers for DS-CDMA systems", Proc. The 11th IEEE International Symposium on Personal, Indoor, and Mobile Radio Communications (PIMRC), London, Sep. 2000.

[54] T. Ristaniemi, "Synchronization and blind signal processing in CDMA systems", Ph.D. thesis, University of Jyväskylä, Finland, 2000.

[55] T. Ristaniemi, J. Joutsensalo, "Advanced ICA-based receivers for block fading DS-CDMA channels", Signal Processing, vol. 82, pp. 417-431, Mar. 2002.

[56] R. Roy, T. Kailath, "ESPRIT-estimation of signal parameters via rotational invariance techniques", IEEE Trans. on Acoustics, Speech, and Signal Processing, vol. 37, pp. 984-995, Jul. 1989.

[57] R. Roy, B. Ottersten, L. Swindlehurst, and T. Kailath, "Multiple invariance ESPRIT", IEEE Trans. on Acoustics, Speech, and Signal Processing, vol. 40, pp. 867-881, Apr. 1992.

[58] R. Roy, T. Kailath, "ESPRIT - Estimation of signal parameters via rational invariance techniques," IEEE Trans. on Acoustics, Speech, Signal Processing, vol. 37, pp. 984-995, Jul. 1989.

[59] A.A.M. Saleh, R. Valenzuela, "Mobile Radio Communications", Pentech, London, 1992.

[60] R.O. Schmidt, "Multiple emitter location and signal parameter estimation", IEEE Trans. on Antennas and Propagation, vol. 43, pp. 276-280, Mar. 1986.

[61] T. Shen, M. Wax, and T. Kailath, "On spatial smoothing of direction-of-arrival estimation of coherent signals", IEEE Trans. on Acoustics, Speech, and Signal Processing, vol. 33, pp. 806-811, Aug. 1985.

[62] P. Stoica, A. Nehorai, "MUSIC, maximum likelihood, and Cramer-Rao bound", IEEE Trans. on Acoustics, Speech, and Signal Processing, vol. 37, pp. 720-741, May 1989.

[63] P. Stoica, A. Nehorai, "MUSIC, maximum likelihood, and Cramer-Rao bound: further results and comparisons", IEEE Trans. on Acoustics Speech, and Signal Processing, vol. 38, pp. 2140-2150, Dec. 1990.

[64] P. Stoica, A. Nehorai, "Performance study of conditional and unconditional direction-of-arrival estimation", IEEE Trans. on Acoustics, Speech, and Signal processing, vol. 38, pp. 1783-1795, Oct. 1990.

[65] P. Stoica, K.C. Sharman, "Novel eigenanalysis method for direction estimation," IEE proceedings F, vol. 137, pp. 19-26, 1990.

[66] P. Stoica, R.L. Moses, "Introduction to spectral analysis", Prentice Hall, Englewood Cliff, New Jersey, 1997.

[67] E.G. Strom, S. Parkvall, S.L. Miller, and B.E Ottersten, "Propagation delay estimation in asynchronous direct-sequence code-division multiple access systems", IEEE Trans. on Communication, vol. 44, pp. 84-93, Jan. 1996.

[68] E.G. Strom, S. Parkvall, S.L. Miller, and B.E Ottersten, "DS-CDMA synchronization in time-varying fading channels", IEEE Journal Selected Areas Communication, vol. 14, pp. 1636-1642, Oct. 1996.

[69] E.G. Strom, F. Malmsten, "A maximum likelihood approach for estimating DS-CDMA multipath fading channels", IEEE Journal on Selected Areas in Communications, vol. 18, pp. 132 -140, Jan. 2000.

[70] W.L. Stutzman, G.A. Thiele, "Antenna theory and design", John Wiley & Sons, New York, 1981

[71] M.C. Vanderveen, C.B. Papadias, and A. Paulraj, "Joint angle and delay estimation (JADE) for multipath signals arriving at an antenna array", IEEE Communications Letters, vol. 1, pp. 12 -14, Jan. 1997.

[72] M.C. Vanderveen, A.-J. Van der Veen, and A. Paulraj, "Estimation of Multipath Parameters in Wireless Communications", IEEE Trans. on Signal Processing, vol. 46, pp. 682-690, Mar, 1998.

[73] A.-J. Van der Veen, M.C. Vanderveen, and A. Paulraj, "Joint angle and delay estimation using shift-invariance properties", IEEE Signal Processing Letters, vol. 4, pp. 142 -145, May 1997.

[74] A.-J. Van der Veen, M.C. Vanderveen, and A. Paulraj, "Joint angle and delay estimation using shift-invariance techniques", IEEE Trans. on Signal Processing, vol. 46, pp. 405-418, Feb. 1998.

[75] S. Verdu, "Multiuser detection", Cambridge University Press, New York, 1998.

[76] A.J. Viterbi, "CDMA : Principles of Spread Spectrum Communication", Prentice Hall PTR, 1995.

[77] M. Viberg, "Subspace fitting concepts in sensor array processing", Ph.D. thesis, Linkoping University, Sweden, 1989.

[78] M. Viberg, B. Ottersten, "Sensor array processing based on subspace fitting", IEEE Trans. on Signal processing, vol. 39, pp. 1110-1121, May 1991.

[79] M. Viberg, and B. Ottersten, and T. Kailath, "Detection and estimation in sensor arrays using weighted subspace fitting", IEEE. Trans. on Signal Processing, vol. 39, pp. 2436-2449, Nov. 1991.

[80] K. Wang, H. Ge, "Joint Space-Time Channel Parameter Estimation for DS-CDMA System in Multipath Rayleigh Fading Channels", Electronics Letters, vol. 37, pp. 458-460, Mar. 2001.

[81] Y.Y. Wang, J.T. Chen, and W.H. Fang, "TST-MUSIC for joint DOA-delay estimation", IEEE Trans. on Signal Processing, vol. 49, pp. 721 -729, Apr. 2001.

[82] M. Wax, A. Leshem, "Joint estimation of time delays and directions of arrival of multiple reflections of a known signal", IEEE Trans. on Signal Processing, vol. 45, pp. 2477-2484, Oct. 1997.

[83] J. H. Wilkinson, "The Algebraic Eigenvalue Problem", Oxford University Press, New York, 1965.

[84] G. Xu, S.D. Silverstein, R.H. Roy, and T. Kailath, "Beamspace ESPRIT", IEEE Trans. on Signal Processing, vol.42, pp. 349-356, Feb. 1994.

[85] X.-L. Xu, K.M. Buckley, "Bias analysis of the MUSIC location estimator", IEEE Trans. on Signal Processing, vol. 40, pp. 2559-2569, Oct. 1992.

[86] Q.T. Zhang, "Probability of resolution of the MUSIC algorithm", IEEE Trans. on Signal Processing, vol. 43, pp. 978-987, Apr. 1995.